Establishing the relationships between the CSM LAI and yield with backscatter value Satellite images: A case study over the Northern Karnataka

Chandrakant Raj H
Tamil Nadu Agricultural University
Boomiraj Kovilpillai
kb78@tnau.ac.in
Tamil Nadu Agricultural University
Pazhanivelan S
Tamil Nadu Agricultural University
Sathya Moorthy N K
Tamil Nadu Agricultural University
Prasanthrajan M
Tamil Nadu Agricultural University
Sudarmanian N S
Tamil Nadu Agricultural University
Satheesh S
Tamil Nadu Agricultural University
Sangeethapiriya R
Tamil Nadu Agricultural University
Karthikeyan G
Tamil Nadu Agricultural University
Gayathri J
Anna University, Chennai

Research Article

Keywords: LAI, biophysical model, backscattering (dB), InfoCrop, and CERES

Posted Date: December 4th, 2024

DOI: https://doi.org/10.21203/rs.3.rs-5384946/v1

Additional Declarations: No competing interests reported.

Abstract

India's extensive agrarian and aerospace research systems offer numerous potential technologies suited for the crop insurance sector. This study investigates the application of technology in domains such as yield prediction, loss assessment, and product design. The research was conducted in the Vijayapura, Karnataka by integrating an intrinsic bio-physical model with remote sensing. As the agricultural statistics play major role in shaping the strategies and plans under food security, an area of 51,482.3 ha was estimated using SAR data, achieving an accuracy of 87.2% and a kappa index of 0.74. Indigenously developed InfoCrop and SORGHUM- CERES were employed to estimate yield for selected monitoring locations, with simulated LAI and yield ranging from 2.6 to 4.65 and 749 to 1097 kg ha^{-1}, respectively. When compared with observed data, results showed an agreement above 90% and RMSE less than 10% and R^2 above 70%. Using regression ($R^2 > 0.75$) equations [CSM’s LAI and backscattering (Db)] and [spatial LAI and CSM yield], LAI and yield maps were developed.

1. INTRODUCTION

Among cereal crops grown widely across India Jowar *(Sorghum bicolor)* (Sandeep *et al.*, 2017) holds significant value due to its adaptability to a wide range of agroclimatic environments. (Srivastava *et al.*, 2010) with a few exemptions in Northern India, sorghum is mostly grown as a dryland breakfast cereal crop in the Deccan Plateau, Central, and Western regions of India. It is more nutritious than other small grains like wheat and rice because of its substantial mineral content, delayed digestion, and high level of fibre. Due to its usual cultivation on nutrient-poor soils in often drought-prone areas, sorghum reduces risk and hence promotes food and feed security (Boomiraj *et al.*, 2012; Murty *et al.*, 2007). As well as its economic worth is matched by its nutritional importance, making it one of the most crucial components of our nation's agricultural landscape. (Naresh Kumar *et al.*, 2014) India being the world's fifth-largest producer of sorghum, has a vital stance for meeting domestic consumption demands (Sandeep *et al.*, 2017). Since 1991, the mean yield data of sorghum is in a non-significant increasing trend with the highest production observed in the years 2021, 2008, and 2020. This cereal is seen in the decreasing trend of harvested area from 13.041 m ha to 4.093 m ha with a trend value of $R^2 = 0.97$ globally (FAOSTAT, 2023). Thus, well-established techniques for estimating the area and production of crops must be created both nationally and internationally.

Despite India's extensive agrarian and aerospace research system, which has many potential technologies suited for the insurance sector, there have been only a few fragmentary studies on the application of technology in domains like yield prediction, loss assessment, and product design. Agriculture statistics are essential for establishing agricultural plans and strategies, as well as for coordinating and allocating resources to support the growth of the agricultural industry (Aggarwal *et al.*, 2016). A timely and non-destructive assessment is required for the crop yield forecast of the remote sensing which is acquired by the which is possible by unmanned aerial vehicles through the spatial-temporal approach on the imagery scale (Zhou *et al.*, 2017). Accurate crop forecasting may become a strategy for guaranteeing food security in the current scenario of changing climate, growing susceptibility, and food insecurity. For several user groups, such as agricultural planners and policy makers, crop insurance firms, and the research community, early yield assessment at regional and national sizes is becoming more crucial (Dubey *et al.*, 2018). Several methods have been developed by the different sectors in agriculture for yield estimation such as statistical approach, (Lobell and Burke, 2010) Satellite-based approach (Burke and Lobell, 2017) and as data assimilation of crop models into the remote sensing (Jin *et al.*, 2018) as because the biophysical crop models cannot represent the outputs at geospatial or large levels (Wagner *et al.*, 2020).

At granular level in Indian condition many models like InfoCrop (Aggarwal *et al.*, 2006a; Boomiraj *et al.*, 2012; Byjesh *et al.*, 2010; A. Kumar *et al.*, 2015) DSSAT (Anusha *et al.*, 2023, 2023; Parmar *et al.*, 2013; Subash and Mohan, 2012), APSIM (Mohanty *et al.*, 2012), CERES (Singh *et al.*, 2017), AquaCrop (Singh *et al.*, 2013; Umesh *et al.*, 2022), ORYZA (Li *et al.*, 2011) and have proven to be successfully simulated for growth parameters, yield and climate change yield prediction other than these satellite data driven methods are also famous for the crop monitoring and the yield prediction (Dadhwal *et al.*, 2003; Thirumeninathan *et al.*, 2023). The effective benefits under this remote can be given as (i) spatial yield estimation in different seasons which can be current and past (ii) an efficient analysis can be done with low-price remote sensing products such sentinel- 1A data which is freely available (iii) an all-time available data available for delineating the crops (Mosleh *et al.*, 2015). Researchers have developed the mono-temporal or multi-temporal inputs for the estimation of crops through satellite imagery but it's quite difficult to get the cloud free images that too in the important stages of crop which have to accurately match with the LAI. (Batchelor *et al.*, 2002; Karydas *et al.*, 2015; Quarmby *et al.*, 1993).

Hence, in the contemporary scenario, a proper coupling of the empirical models, statistical models, and crop simulation models to remote sensing is to be done for the proper estimation of the crop yield even though, remote sensing is formally accepted for the estimation of area and estimation biomass by LAI which is yet to be developed by researchers, so here comes crop simulation models which can stand an outstanding support system for yield predictions by providing the numerous growth parameters such as LAI (Brogi *et al.*, 2020; Gumma *et al.*, 2022; Pandya *et al.*, 2006; Pazhanivelan *et al.*, 2022; Su *et al.*, 2015; Thirumeninathan *et al.*, 2023) and yield (Bhatia *et al.*, 2005; Yadav *et al.*, 2012). Lack of adequately accurate input data, such as parameter values for soil, management, cultivar, and climatic inputs, frequently renders it difficult to simulate cropping systems efficiently. However, merging these two methods may allow cropping system model simulations to be updated and more certain results might be obtained (Lobell *et al.*, 2015; Nearing *et al.*, 2012; Potgieter *et al.*, 2021). In this study, we have developed crop parametric data with the intrinsic biophysical simulation model like the Decision Support system for Transfer of Agro-technology (DSSAT) (Jones *et al.*, 2003) and InfoCrop (Aggarwal *et al.*, 2006) and assimilated these in remote sensing data to create Leaf Area Index (LAI) and yield map spatially.

2. SELECTION OF SITE DESCRIPTION OF STUDY AREA

India is the fifth largest producer of sorghum; the *rabi* sorghum has shown the highest area and production under this crop in Maharashtra followed by Karnataka, Tamil Nadu, Andhra Pradesh and

Telangana (Saxena *et al.*, 2019) as statistical data depicts the productivity per hectare of Andhra Pradesh and Telangana have the highest this could be anticipated for better irrigation facilities while compared to Maharashtra and Karnataka are lowest in their productivity even though area is higher. Among the aforementioned states the district is Vijayapura, Karnataka as the state statistics have shown the decrease in the area i.e., as low as 50% of winter sorghum in this particular area from the year 2019-20 to 2020-21. (Anonymous(a),2021). Vijayapura is located in the northern part of Karnataka as well as India's northern Deccan plateau region Fig. 1. of almost arid to semi-arid climate which mostly experiences hot summers and majority of rainfall from the summer monsoon with moderate winters that has feasible rainfall makes the farmers go for drought-resistant crops for the production which makes sorghum a unique cereal and other millets; whereas region is mostly deep black soils which have little water infiltrations so it makes sorghum farmer favourite crop in these regions. Karnataka’s lowest rainfall was seen in Vijayapura region of 579mm and other thirteen talukas namely Bijapur, Indi, Sindagi, Basavana bagewadi, Muddebihal, Nidagundi, Babaleshwara, Chadchana, Talikote, tikota, Kolhara, Devara Hipparagi, Alamela have received rainfall ranging from 565 to 635 mm in that almost 60% from normal monsoon (Jun-Sept); 23% is from post monsoon (Oct-Nov) and lastly 14% from pre-monsoon (Apr-may) as per the (Anonymous(b),KVK report 2021).

3. Materials and methods

3.1. Using remote sensing in conjunction with CSM models to estimate crop production:

Many literatures have shown the high correlation of LAI with yield and other attributes such as yield in cotton (Hashimoto et al., 2023; Li et al., 2022) and rice (Aboelghar et al., 2011) evapo-transpiration in the apple orchards (Jia and Wang, 2021), disease infestation- sun flower (Leite et al., 2006) and even the nitrogen accumulation (LIU et al., 2018) of the plants in the plant growth and simulation. So, satellite products can’t give the direct values of the LAI so simulation models are used for the LAI prediction and later the relationship between the LAI and backscatter was found so a detailed methodology of the assessment is given in the Fig. 2 and for the collection of ground truthing the prediction of LAI and yield is given in detailed.

3.2 Ground truth data collection for training and validating data and monitoring sites data such LAI, Soil, Management practices and yield:

Strenuous efforts have been made in the collection of the ground truthing during *December 2022* for the crop sown locations which were taken up for every 2–5 km with a protocol of homogenous cropland of 1 ha which is 50 m away from the road, built infrastructures (Raviz *et al.*, 2015) and in *February 2023* collection of yield data from the farmers. An overall proportionate journey covering overall 600 km almost 150 *rabi* sorghum points and 100 non- sorghum points were collected. Ground truthing involved selecting five plants randomly at each monitoring site to assess the Leaf Area Index (LAI) and for crop simulation models. LAI calculations were based on phenological and physiological mechanisms, measured by the length and width of the fully expanded third tetra-foliate leaf from 30 Days After Sowing (DAS) to harvest.

$$LAI = \frac{L\ x\ W\ x\ 0.70x\ number\ of\ leaves}{Spacing\ (cm)}$$

L = Length of the top third leaf of the plant, W = Width of the top third leaf of the plant & K-Constant factor (0.70). Average LAI was calculated from measurements taken from six to ten leaves in each field. Yield data were collected at the end of the growing season. Ground truth data also include the LAI and yield from the 25 monitoring sites Fig. 3 **&** Table 1. The management practices from the monitoring sites such as water management, crop cultivars, and soil properties were taken for observational purposes.

Table 1
Observed Leaf Area Index and Yield for monitoring sites

ID	Village	District	Lat	Long	LAI	Yield (kg ha^{-1})
1	Benakanahalli	Vijayapura	17.00	75.95	3.95	1080
2	Honnalli	Vijayapura	16.96	75.91	3.48	1049
3	Shivanagi	Vijayapura	16.79	75.98	3.10	749
4	Nagatana	Vijayapura	16.95	75.87	3.80	936
5	Dhanargi	Vijayapura	16.86	75.6	4.12	1097
6	Thajapura H	Vijayapura	16.78	75.53	3.84	942
7	Babaleshwara	Vijayapura	16.68	75.63	3.75	945
8	Honaganahalli	Vijayapura	16.68	75.7	3.85	1037
9	Managoli	Vijayapura	16.67	75.75	3.71	875
10	Donara	Vijayapura	16.72	75.96	3.47	928
11	Basavana Bagewadi	Vijayapura	16.63	75.91	3.85	907
12	Mutthagi	Vijayapura	16.57	75.89	3.80	931
13	Devura	Vijayapura	16.25	76.12	3.75	978
14	Basarakoda	Vijayapura	16.39	76.1	3.65	962
15	Madike Shirura	Vijayapura	16.5	76.18	4.00	1002
16	Sindhageri	Vijayapura	16.64	76.18	3.50	877
17	Fathepura .P.T	Vijayapura	16.56	76.32	3.80	945
18	Kalakeri	Vijayapura	16.66	76.3	3.60	995
19	Thalikote	Vijayapura	16.5	76.34	3.65	1007
20	Ukkali	Vijayapura	16.7	75.91	4.30	1036
21	Sindhagi	Vijayapura	16.9	76.28	3.65	877
22	Chandakawati	Vijayapura	16.95	76.16	3.30	860
23	Devara Hipparagi	Vijayapura	16.78	76.03	3.10	953
24	Yalavara	Vijayapura	16.69	76.09	3.20	889
25	Sarawada	Vijayapura	16.74	75.66	4.00	1006

Table 2
Sentinel 1A data acquisition dates - rabi season, 2022-23

S. No.	Satellite Pass	Acquisition Date
1	D_1	29.08.2022
2	D_2	10.09.2022
3	D_3	22.09.2022
4	D_4	04.10.2022
5	D_5	16.10.2022
6	D_6	28.10.2022
7	D_7	09.11.2022
8	D_8	21.11.2022
9	D_9	03.12.2022
10	D_{10}	15.12.2022
11	D_{11}	27.12.2022
12	D_{12}	08.01.2023
13	D_{13}	01.02.2023
14	D_{14}	13.02.2023
15	D_{15}	25.02.2023

3.3. Collection of the Sentinel-1A data sets:

Sentinel-1A -SAR have got great momentum in last decade for its ability to monitor crop biomass under which the C-band has high impact in the for estimation of the crop biomass monitoring (Parag *et al.*, 2023), which has many advantages like twin satellite so for every 6-day revisit and freely availability (Harfenmeister *et al.*, 2021) so for the monitoring of remote sensing almost 12-day interval **Table. 2**, which works on different wavelengths that has ability to go through clouds and facilitating in day and night opportunities for collection which is European radar mission co-jointly ventured by European commission and European space Agency (Liu *et al.*, 2019) and this satellite imagery data for which has the fluent and charge free accessibility through https://scihub.copernicus.eu/dhus/ the images' have downloaded from the time period as scheduled in crop calendar which was created for the *rabi* sorghum in *2022-23* Fig. 4. It has ground range coverage of almost 251.8 kms and selected a VH polarization Interferometric Wide (IW) swath, and wave modes, each with different resolutions and coverage areas.

3.3.1. Spatio-temporal image process:

Streamlining processes and compressing the timeline of vast datasets is a time-consuming process which has been tackled by the automated chain process a string module which is present in MAPscape-RICE a software, which was developed by SAR-map, Switzerland. A time-series SAR data have streamed through different process such as strip mosaicking, co-registration, time- series speckle filtering, terrain geocoding, ANLD filtering, removal of atmospheric attenuation and sub-setting a detailed flowchart in Fig. 5 So, when it's in estimating area over multi-layer temporal image process a rule- based classifier has been made for quick persistent experimentation for the selected monitoring sites to keep engaging in temporal signatures to match with crop stages for this degree of expertise is required in setting up the other sources and information and to further guide parametric values.

3.4. Crop categorization and Accuracy:

3.4.1. Maximum likelihood classification:

In the earlier stage of the study, a detailed explanation was provided regarding the methodology series employed for preprocessing Sentinel-1A images with a focus on handling multi-temporal values. The procedure involved using an algorithm based on Maximum Likelihood Classification. During this process, a training dataset was utilized, and statistical parameters, specifically the mean vector and covariance matrix, were estimated assuming a Gaussian distribution. In more detail, the mean vector represents the average values of the dataset in a vector format, capturing the central tendency of the data. The covariance matrix, on the other hand, encapsulates the variability and relationships between different components of the dataset. These statistical parameters were calculated to effectively model the underlying distribution of the data. This approach assumes that the data follows a Gaussian distribution, and by utilizing the mean vector and covariance matrix, it is presumed that these statistical descriptors can adequately represent the entire dataset. To identify *Rabi* sorghum in the image, an initial classification was performed using Maximum Likelihood Classification (MLC), incorporating multi-temporal Synthetic Aperture Radar (SAR) images superimposed on each other. Training pixels were obtained from diverse locations, and these were used to establish the spectral signature specific to *Rabi* sorghum. Subsequently, the classification process was specifically carried out for the Vertical-Horizontal (VH) polarization, aiming to differentiate *Rabi* sorghum fields from other land cover categories.

3.4.2. Accuracy Validation:

In the land assessment techniques researchers (Bolstad and Lillesand, 1992; Murthy *et al.*, 2003) frequently employ the Kappa statistic and associated statistical methods to evaluate the reliability of classifications derived from remote sensing data. This involves constructing an error matrix that systematically documents pixels indicating agreement and disagreement between classified and reference datasets.

To validate the following survey which conducted during the early vegetative stages to ensure the post-harvest rabi crop presence in the field. Overall accuracy was calculated as the sum of correctly classified classes along the diagonal divided by the sum of row or column totals. Ground truthing accuracy for each class was determined by dividing the total correctly categorized samples by the total reference samples. User accuracy (errors of omission) for each class is the percentage of correct classifications out of the total samples checked in that class.

User's accuracy = $\frac{\text{Number of correctly classified class in a row}}{\text{Total Number of items verified in that row}}$

The Kappa coefficient, an alternative metric for classification accuracy, was calculated using the where A is the sum of diagonal elements (numerator for overall accuracy calculation), B is the sum of products of row and column totals, and N is the total number of pixels in the error matrix.

$$K = \frac{NA - B}{N^2 - B}$$

3.5. Inputs for CSM:

3.5.1. Locations based-weather Data:

Any biophysical-based model to anticipate the growth of the heat units is required to define different growing stages along with the effects of different weather parameters on yield hence, daily weather data such as maximum temperature (°C), minimum temperature (°C), solar radiation (MJ m^{-2} day^{-1}) and rainfall (mm) for Rabi 2022–2023 of the particular locations of Vijayapura has been taken archives of the (NASA POWER project, 2023).

3.5.2. Soil Data for Crop Simulation:

It is difficult to obtain at such a granular level of global soil data when using limited soil-gridded data for crop simulation. Hence, ISRIC-AfSIS have created a DSSAT-compatible soil profile on a 5 arc-minute grid that incorporates important soil attributes (bulk density, organic carbon, percentage of clay and silt, soil pH and cation exchange capacity) using soil-grids with spatial resolution (Hengl *et al.*, 2014) of 1km.

The soil data in InfoCrop program was made previously from the soil database for India and was taken from NBSSLUP at a 1:250,000 scale providing soil series information for 60 agroecological subregions of India. The characteristic data of major soil types in a grid (1° × 1°) were extracted using GIS tools and entered into the model (Naresh Kumar *et al.*, 2014). Based upon the soil field observation and availability were selected for the model running.

3.5.3. Field Crop Management practices:

A database was created during the survey of the district for collection of the crop management details mainly including sowing window, crop cultivars, water management (techniques on/off options), fertilizer management (water and nitrogen balances), depending upon the survey condition and continuous contact with farmers the crop yield data was taken up. DSSAT provides an X-Build tool that helps in the management and calibration of the file as well; InfoCrop is a simple tool that helps to stimulate growth with inputs sowing dates, soil file, water and fertilizer management techniques.

3.5.4. Opting for specific crop strains and deriving genetic coefficients:

The crop cultivars is to perform in simulating crop growth and yield so the selection of the crop variety was based upon the literature (A. A. Kumar *et al.*, 2015; Nagaleekara *et al.*, 2023) Anonymous(b),KVK report 2021) and farmers advise; as well as KVK scientist recommendation four varieties were selected to match the crop grown in *Rabi* season for growth and production and simulation in namely M35-1 a farmer favourite variety and famously known as Maldandi; BJV-44, CSV-29R and CSH-16 the description of genetic co-efficient are further explained in results and genetic co-efficient given in the Annexure table.

3.6. Statistical evaluation and validation of products

The yield of sorghum crops was estimated using remote sensing products integrated with the DSSAT model and compared to the actual yield observed in the field. To assess the agreement between estimated and observed values, R^2, Root Mean Square Error (RMSE), Normalized Root Mean Square Error (NRMSE), and agreement percent were calculated. R^2 indicated the percentage of variation in estimated yield explained by observed yield. RMSE and NRMSE measured the magnitude of differences between estimated and observed yields, with NRMSE providing a scale-adjusted comparison. Agreement percent showed the similarity between the two sets of values, demonstrating the precision of the integrated estimation method.

RMSE = $\sqrt{1/N \sum\ (Oi - Pi)^2}$

NRMSE = 100 x (RMSE / Oi)

Agreement (%) = 100 x (1- (RMSE / Oi))

4. Results and Discussion

4.1. Rabi sorghum area assessment and its accuracy:

4.1.1. Temporal Analysis of VH Polarization Backscattering for Rabi Sorghum Crop Identification:

The VH polarization signature curve of Rabi sorghum exhibited a noteworthy increase of -23.65 dB from the seedling to the vegetative stage, succeeded by a gradual incline to -16.81 dB during panicle development. Subsequently, at maturity, there was a decline to -22.97 dB, as visually depicted in Fig. 6. Based upon these, a similar pattern of multitemporal data within the pixel a thematic map was developed and presented for the crop maximum likelihood classification information which was extracted from SAR data for rabi sorghum for the Vijayapura District talukas, while administrative boundary shapefiles were used from Karnataka State Remote Sensing Applications Centre, Bengaluru in a clear and easily understandable way. The classified *Rabi* sorghum area in the Vijayapura district was assessed to be 51,482.3 ha. Figure 7. Among thirteen talukas in Vijayapura district, the highest *Rabi* sorghum area was recorded in Basavana Bagevadi with an area of 12655 ha block followed by Babaleshwara and Devara Hipparagi with an area of 7043.5 ha and 6042.32 ha, respectively. While lowest was seen under Chadchana and Alamela talukas with an area of 484.8 and 84.072 ha of *Rabi* sorghum area, respectively Table 3. Based on the presented data and subsequent crop area assessment, it has been confirmed that a substantial portion of the region has undergone a reduction in the area allocated to *rabi* sorghum cultivation. (Anonymous(b), KVK report 2021), sourced from which Basavana Bagewadi, Vijayapura, Mudebihal, and Sindagi, reveals this trend.

Table 3
Statistics block wise Rabi sorghum area for Vijayapura

S.no	Taluka	Area(ha)	Percentage
1	Bijapur	4468.9	8.68
2	Indi	2837.9	5.51
3	Sindagi	1728.7	3.36
4	Basavan Bagewadi	12655.0	24.58
5	Muddebihal	5619.8	10.92
6	Nidagundi	1069.6	2.08
7	Babaleshwara	7043.5	13.68
8	Chadachana	484.8	0.94
9	Talikote	3926.2	7.63
10	Tikota	4582.9	8.90
11	Kolhara	938.1	1.82
12	Devara Hipparagi	6042.3	11.74
13	Alamela	84.0	0.16
Total		**51482.3**	**100.00**

4.2. Level of precision in Area assessment

For the *Rabi* sorghum area map, a comprehensive evaluation was undertaken, leveraging ground truth points obtained from both the Rabi sorghum and non-sorghum regions. This validation process encompassed the collection of 135 points representing Rabi sorghum and 15 points from non-sorghum areas within the designated study region. The outcomes of this evaluation unveiled that the Rabi sorghum area map exhibited an overall accuracy of 87.2%; Furthermore, the calculation of the kappa index, classification accuracy, yielded a value of 0.74. This value indicates an estimation accuracy for the Vijayapura district during the Rabi season of 2023, Table 4. and after the assessment of the accuracy of the crop classification an crop mask area is generated Fig. 7.

Table 4
Confusion matrix for accuracy assessment for sorghum crop classification during *rabi* 2022-23

Actual class from accuracy	Predicted class from map			
	Class	**Sorghum**	**Non-Sorghum**	**Accuracy (%)**
	Sorghum	**135**	**15**	**88.7%**
	Non-Sorghum	**15**	**85**	**85%**
	Reliability	**89.9%**	**83.3%**	**87.2%**
Overall accuracy				87.2%
Kappa index				0.74

4.3. Generation of genetic co-efficient for Rabi Sorghum under Vijayapura region:

The development of genetic coefficients for the Vijayapura region, specifically in the context of spatial calibration, represents a crucial advancement in genetic research. Genetic coefficients play a pivotal role in understanding the heritability and genetic variability of traits within a given crop variety. Under this article establishing relations between the LAI and backscatter the derivation of genetic coefficients is crucial which change spatially and needs calibration to different environment, we aim to refine and customize these coefficients based on the geographical characteristics of the Vijayapura region. This involves accounting for the spatial heterogeneity of environmental factors that influence genetic expression the genetic co-efficient are presented in **annexure Table** for both the Decision Support System for Agrotechnology Transfer (DSSAT) and InfoCrop. The results of the simulated and observed LAI and yield show a good R-value > 0.70.

4.4. Obtaining Leaf Area Index (LAI) from relation between SAR-Db and CSM LAI

After validating the simulated and observed LAI and Yield from the CSM with $R^2 > 0.7$ then they were subjected to further process. From the obtained multi-temporal dataset, a peak dB (backscattering) values were obtained for the monitored fields and peak LAI from CSM were taken and subjected to for the creation of a linear regression **(Eqs. (1 and 2)**) and Figs. 8 & 9. The spatial LAI -map was generated for the study region with equations **Figs. 10 & 11.**

LAI= -0.36*db-2.31 (DSSAT) — (1)

LAI= -0.53*dB-5.97 (InfoCrop) ——(2)

4.4.1. Sorghum yield estimation based on remote sensing

After validation of the yield from the model to observed value. The CSM's simulated yield was integrated with the spatial LAI values i.e., values extracted from the above process a linear regression was run Figs. 12 & 13 which was developed and for running spatially to obtain sorghum yield for the research area. Finally obtained equation are **Eqs. (3 and 4)** were subjected to map- algebra module of ArcGIS for Spatial Yield maps

Yield = 200.06*LAI + 133.63 (DSSAT) –(3)

Yield = 195.13*LAI + 162.83 (InfoCrop) —(4)

4.5. Generation of LAI and Yield maps and area statistics Table at the taluka level:

After the generation of a good correlation of above 70% with SAR-Db and model LAI the regression equation was placed in ArcGis software map algebra tool to generate the individual Spatial LAI maps for the DSSAT and InfoCrop were generated **Figs. 10 & 11** and area statistics was ran over the assessed area for getting LAI Table 5. Later, the same monitoring site-specific Spatial LAI- Model yield was under gone a regression Figs. 12 & 13 then the regression equation was placed in ArcGis software map algebra tool to generate the individual yield-maps for the DSSAT and InfoCrop Figs. 14 & 15. Area statistics was run over the assessed area for getting spatial yield statistics **Table 6.**

Table 5

Depiction of the LAI of crop after regression relation between Db-CSM LAI

S.no	Taluka	DSSAT-LAI			RS-LAI		
		MIN	MAX	MEAN	MIN	MAX	MEAN
1	Bijapur	1.6	6.1	4.4	2.9	5.0	3.7
2	Indi	1.3	6.0	4.4	2.9	5.2	3.7
3	Sindagi	2.5	6.1	4.5	2.9	4.6	3.6
4	Basavan Bagewadi	1.3	6.2	4.4	2.8	5.4	3.7
5	Muddebihal	2.6	6.6	4.5	2.6	4.5	3.6
6	Nidagundi	2.6	6.3	4.7	2.8	4.5	3.5
7	Babaleshwara	2.0	6.3	4.4	2.8	4.8	3.7
8	Chadachana	2.5	6.0	4.5	2.9	4.6	3.6
9	Talikote	1.8	6.1	4.4	2.9	4.9	3.7
10	Tikota	1.6	7.1	4.6	2.4	5.0	3.6
11	Kolhara	2.5	5.9	4.2	3.0	4.6	3.8
12	Devara Hipparagi	2.5	6.3	4.3	2.8	4.6	3.7
13	Alamela	3.0	5.8	4.4	3.0	4.4	3.7

Table.6 Depiction of the yield crop after regression relation between Db-LAI & CSM yield

S.no	Taluka	DSSAT-YIELD (Kg/ha)			RS-YIELD (Kg/ha)		
		MIN	MAX	MEAN	MIN	MAX	MEAN
1	Bijapur	543	1190	950	624	1043	779
2	Indi	502	1171	952	636	1069	778
3	Sindagi	684	1192	958	623	952	774
4	Basavan Bagewadi	439	1205	949	614	1110	780
5	Muddebihal	695	1267	966	574	945	769
6	Nidagundi	692	1216	992	607	946	752
7	Babaleshwara	601	1219	953	605	1005	777
8	Chadachana	673	1181	968	630	959	768
9	Talikote	570	1193	945	622	1025	782
10	Tikota	545	1335	969	530	1041	767
11	Kolhara	676	1159	919	643	957	799
12	Devara Hipparagi	673	1223	940	602	959	786
13	Alamela	745	1141	951	655	912	779

5. Discussion

The majority crop which grows in the particular study area is rabi season's sorghum through the ground truthing as it is important crop in the dry region major farmers rely on this crop due to arid conditions of the area. MAP-scape advanced techniques for improving the resolution of the images at 20m was possible and the availability of the Gramin GPS etrex10 as it gives the 10 active satellite accurate Global Positioning for the ground truthing as pixel size is very high leaf area index measurement was done by traditional method as the unavailability of canopy analyser still the accuracy of afore mentioned is remarkable as the location of the LAI was known it was easier for the validation of the CSM models for the 25 monitoring a similar approach was followed in rice and peanut crops (Pazhanivelan *et al.*, 2022; Thirumeninathan *et al.*, 2023). The area generated with accuracy of overall 87.24% similar approaches was done measure accurate rice area (Kannan *et al.*, 2021a, 2021b; Ragunath Kaliaperumal *et al.*, 2021; Satheesh *et al.*, 2022; Setiyono *et al.*, 2019); sugar-cane (Selvaraju *et al.*, 2019) and peanut (Thirumeninathan *et al.*, 2023). However, it is noteworthy that pockets within the Indi block still exhibit the cultivation of *rabi* sorghum. The Vijayapura region, as indicated in the report in KVK, has witnessed a diminishing trend in sorghum cultivation, with farmers increasingly favouring major *rabi* crops like chickpea and wheat over the preceding five years. This transition is primarily linked to enhanced profitability associated with these crops, which command higher market prices and ensure a more sustainable income for farmers. The decline in sorghum cultivation is further elucidated by challenges such as the absence of mechanized equipment for harvest processing, contributing to diminished yields and unfavourable market prices *Boomnalli (2023)*

The temporal datasets of the given ground truthing points, an analysis showed a substantial rise of 1.69 dB from – 18.85 at the season's commencement to -16.81 during the seedling stage. Considering the entire growth cycle of Rabi sorghum, the VH polarization backscattering exhibited maximum and minimum dB values of -23.65 and – 16.81 dB, respectively. Analysing changes in dB values under VH polarization, a noteworthy increase of 0.72 dB was observed from – 23.65 at the season's onset to -22.93 during the seedling stage. Further, a prominent rise of 1.49 dB from D4 to D6 during the vegetative stage was noted, followed by an incremental change of approximately 2.12 dB between D6 and D7. The backscattering gradually increased until the mature stage at D10, with incremental dB rises of 0.19 and 0.69 from D7 to D8 and D8 to D9, respectively a similar approach was followed in rice and peanut crops (Pazhanivelan *et al.*, 2022; Thirumeninathan *et al.*, 2023) to take similar crop pixels from the given multi-temporal dataset of different crops. In this study VH polarization was taken up as it has high sensitivity to the terrain slope and crop characteristics could be useful for the validation of the LAI of the crop a similar approach study was seen in the soyabean and maize (Hosseini et al., 2015) in C and L band.

Decision Support System for Agrotechnology Transfer (DSSAT) and InfoCrop are traditionally to estimate different bio-physical parameters for the crop in which the Genetic co-efficient play a major role for simulating different phenotypic characters for the crop and climate change studies (Boomiraj *et al.*, 2011; Khobragade *et al.*, 2023; Murty *et al.*, 2007; Nagaleekara *et al.*, 2023; Sandeep *et al.*, 2018; Thirumeninathan *et al.*, 2023) which are designated for the geographical areas, recognizing the essential need to accommodate variations in unique environmental factors at each specific location. Here, instead of relying on constant values for genetic factors, this study has taken up a range of genetic coefficients to precisely capture the nuanced environmental influences at distinct spatial points these helped a range of yield outputs that could validate with different observed yield

The research identified a distinctive impact on productivity within the Vijayapura region, and the exact numerical value of the productivity reduction is pending. The models employed in this study simulated LAI using remote sensing products, with rainfall and moisture availability identified as pivotal factors influencing LAI. Model performance, as indicated by the coefficient of determination (R^2) and normalized Root Mean Square Error (nRMSE), demonstrated satisfactory results, with R^2 at 0.75 and nRMSE below 20%. Both CSMs illustrated a robust correlation, exceeding 80%, between LAI and remote sensing products. These findings underscore the significance of integrating CSMs and remote sensing methodologies to comprehend and predict crop yield variations, especially in regions affected by factors such as changing agricultural practices and environmental conditions similar relation between [CSM-based LAI -backscatter values] and [Spatial LAI – CSM Yield] were found in (Pazhanivelan, S.*et al.*, 2008;

Thirumeninathan *et al.*, 2023). A lookup Table was made to make it convenient for the validating the LAI and then yield from the particular location and regression with backscatter value.

The current study was undertaken to underscore the interrelation between Crop Simulation Models (CSMs) and remote sensing methodologies, aiming to obtain a spectrum of crop yields across diverse locations simultaneously. Leaf Area Index (LAI) emerged as a crucial factor in both the spatial distribution of yields and the creation of crop masks for the study area. Numerous investigations revealed a consistent correlation between LAI and yield. Noteworthy observations indicated that achieving a range of yields in a given region necessitates a diverse set of genetic coefficients.

6. Conclusion

This study has showcased the efficacy of integrating remote sensing products with crop models, with a focus on Leaf Area Index (LAI) as the key determinant for yield estimation at the taluka level. The optimization of ground data points encompassed all sorghum-growing areas in the district. The crop mapping achieved an accuracy of 87%, aligning closely with government statistics. Data inputs for the DSSAT and InfoCrop models were gathered during field visits, revealing a substantial overall correlation of 0.80, indicating the model's reliable reflection of field data. The backscattering (dB) from Synthetic Aperture Radar (SAR), a remote sensing product, exhibited a strong correlation with LAI ($R^2 > 80\%$). Consequently, a spatial LAI map was generated, facilitating the creation of a spatial yield map. In conclusion, the integration of remote sensing satellite data with crop models emerges as an effective approach for predicting crop yields, offering valuable insights for policymakers and decision-makers in the implementation of insurance schemes. To conclude the article current study was undertaken to underscore the interrelation between Crop Simulation Models (CSMs) and remote sensing methodologies, aiming to obtain a spectrum of crop yields across diverse locations simultaneously. Leaf Area Index (LAI) emerged as a crucial factor in both the spatial distribution of yields and the creation of crop masks for the study area. Numerous investigations revealed a consistent correlation between LAI and yield. Noteworthy observations indicated that achieving a range of LAI and yields in a given region necessitates a diverse set of genetic coefficients for then establishing a relation between the backscatter values.

7. Future line of work

Models should be taken care of properly and run and calibrated to a big level for incorporating the data sets and bringing the different models that can work in different conditions and a different set of packages in the programming language to be created to run the multi-space and temporal model with the change in the Genetic co-efficient; along with the LAI different variables to be considered for the application for the accuracy of the model outputs. A different set of practices a different LAI and yield and a set of Genetic coefficients with a lookup Table to be considered for precise use of CSMs would develop in the present conditions and can be a game changer for this can reduce the critical time period for yield estimates to harvest dates at different locations. With this, we can conclude it can also be used for future climate change scenario work. So, a different approach like FAPAR, semi-physical methods, machine learning and deep learning to integrate with the CSM and then coupling with the RS products to be taken.

The remote sensing data is purely focussed on the pixel level estimates of the crop or the yield which might not catch the full spectral signature for the area or yield a parcel level (field-size) approach or application should be developed which should be updated yearly due to land fragmented issue and micro level decision of farmer for diversified farming which eventually makes a variation in RS-product and LAI.

Even though the availability of the current dataset with good correlation, many socio-economic attributes might occur which were knowingly or unknowingly not considered and taken as outlier values of yield occurred at the Gram panchayat level so the study was only able to downscale to the sub-level of district(tehsil/taluka). Even though, it was done by recommended a high-resolution (GPS-based) approach for real-time statistical crop yield at the GP level should be maintained or with no bias so it can add value to the commodity markets and planning commission. Globally crop insurance companies and government agencies are focusing on the different or precise methods of early yield prediction of the crop. Still, the crop in the months of the Kharif or Kharif-rabi is not able asses properly due to cloudy data in those seasons and very much price fluctuation was seen in pulses during monsoon of India.

Declarations

Author Contribution

HC, SP, KB and NS and conceptualized the work, analysed the results; HC, KB and NKS drafted the manuscript; NS and SS gave the technical assistance; HC, KB and MP ran the models; HC and SS collected the ground truth; NKS and MP have verified the manuscript. All authors have read and agreed to the published version of the manuscript.

Acknowledgement

This research was supported by the Centre for Water and Geospatial Studies, Tamil Nadu Agricultural University. We would like to thank Dr. S. Pazhnivelan for his support in ground data collection and logistics arrangement.

References

1. Aboelghar, M., Arafat, S., Yousef, M.A., El-Shirbeny, M., Naeem, S., Massoud, A., Saleh, N., 2011. Using SPOT data and leaf area index for rice yield estimation in Egyptian Nile delta. The Egyptian Journal of Remote Sensing and Space Science 14, 81–89.
2. Aggarwal, P., Chand, R., Bhutani, A., Kumar, V., Goel, S., Rao, K., Poddar, M., Sud, U., Krishna Murthy, Y., Ray, S., 2016. Report of the task force on enhancing technology use in agriculture insurance.

3. Aggarwal, P.K., Kalra, N., Chander, S., Pathak, H., 2006a. InfoCrop: a dynamic simulation model for the assessment of crop yields, losses due to pests, and environmental impact of agro-ecosystems in tropical environments. I. Model description. Agric. Syst. 89, 1–25.
4. Aggarwal, P.K., Kalra, N., Chander, S., Pathak, H., 2006b. InfoCrop: a dynamic simulation model for the assessment of crop yields, losses due to pests, and environmental impact of agro-ecosystems in tropical environments. I. Model description. Agric. Syst. 89, 1–25.
5. Anonymous(a),2022. District-wise land use statistics. Directorate of Economics and Statistics, Department of Agriculture and Cooperation, Ministry of Agriculture, Government of India, New Delhi. https://aps.dac.gov.in/LUS/Public/ Reports.aspx
6. Anonymous(b),2022. Krishi Vigyan Kendra, Vijayapura. Annual report 2021-22. https://kvkvijayapura.org/new/wp-content/uploads/2022/12/Annual-Report-2021-22.pdf
7. Anusha, K., Ajithkumar, B., Davis, P.L., Latha, A., Ayyoob, K., Riya, K., 2023. Phasic Development of Rice During the Present and Future Climatic Conditions in Central Zone of Kerala. Int. J. Environ. Clim. Change 13, 26–36.
8. Batchelor, W.D., Basso, B., Paz, J.O., 2002. Examples of strategies to analyze spatial and temporal yield variability using crop models. Eur. J. Agron. 18, 141–158. https://doi.org/10.1016/S1161-0301(02)00101-6
9. Bhatia, V., Singh, P., Wani, S., Srinivas, K., 2005. Yield gap analysis of groundnut in India using simulation modeling. Glob. Theme Agro Ecosyst. Rep.
10. Bolstad, P.V., Lillesand, T.M., 1992. Semi-automated training approaches for spectral class definition. Int. J. Remote Sens. 13, 3157–3166. https://doi.org/10.1080/01431169208904108
11. Boomiraj, K., Marimuthu, S., Wani, S.P., Ravikumar, S., Tani, S., 2012. Vulnerability assessment of kharif rainfed sorghum to climate change in SAT regions of India. J. Agrometeorol. 14, 2–8.
12. Boomiraj, K., Wani, S.P., Agrawal, P., 2011. Impact of climate change on dryland Sorghum in India.
13. Boomnalli, 2023, Manjunath. “Jowar, North Karnataka's staple, sees shrinking cultivation area: ” Deccan Herald, 19th October 2023, https://www.deccanherald.com/india/karnataka/jowar-north-karnatakas-staple-sees-shrinking-cultivation-area-2733136.
14. Brogi, C., Huisman, J., Herbst, M., Weihermüller, L., Klosterhalfen, A., Montzka, C., Reichenau, T., Vereecken, H., 2020. Simulation of spatial variability in crop leaf area index and yield using agroecosystem modeling and geophysics-based quantitative soil information. Vadose Zone J. 19, e20009.
15. Burke, M., Lobell, D.B., 2017. Satellite-based assessment of yield variation and its determinants in smallholder African systems. Proc. Natl. Acad. Sci. 114, 2189–2194.
16. Byjesh, K., Kumar, S.N., Aggarwal, P.K., 2010. Simulating impacts, potential adaptation and vulnerability of maize to climate change in India. Mitig. Adapt. Strateg. Glob. Change 15, 413–431.
17. Dadhwal, V., Sehgal, V., Singh, R., Rajak, D., 2003. Wheat yield modelling using satellite remote sensing with weather data: Recent Indian experience. Mausam 54, 253–262.

18. Dubey, S.K., Gavli, A., Yadav, S., Sehgal, S., Ray, S.S., 2018. Remote sensing-based yield forecasting for sugarcane (Saccharum officinarum L.) crop in India. J. Indian Soc. Remote Sens. 46, 1823–1833.
19. FAOSTAT (2023). Food and Agriculture Organization of the United Nations. http://faostat.fao.org/site/567/default.aspx#ancor (data accessed at 13-06-2023.)
20. Gumma, M.K., Thenkabail, P.S., Panjala, P., Teluguntla, P., Yamano, T., Mohammed, I., 2022. Multiple agricultural cropland products of South Asia developed using Landsat-8 30 m and MODIS 250 m data using machine learning on the Google Earth Engine (GEE) cloud and spectral matching techniques (SMTs) in support of food and water security. GIScience Remote Sens. 59, 1048–1077.
21. Harfenmeister, K., Itzerott, S., Weltzien, C., Spengler, D., 2021. Detecting Phenological Development of Winter Wheat and Winter Barley Using Time Series of Sentinel-1 and Sentinel-2. Remote Sens. 13, 5036. https://doi.org/10.3390/rs13245036
22. Hashimoto, N., Saito, Y., Yamamoto, S., Ishibashi, T., Ito, R., Maki, M., Homma, K., 2023. Relationship between Leaf Area Index and Yield Components in Farmers' Paddy Fields. AgriEngineering 5, 1754–1765.
23. Hengl, T., De Jesus, J.M., MacMillan, R.A., Batjes, N.H., Heuvelink, G.B., Ribeiro, E., Samuel-Rosa, A., Kempen, B., Leenaars, J.G., Walsh, M.G., 2014. SoilGrids1km—global soil information based on automated mapping. PloS One 9, e105992.
24. Hosseini, M., McNairn, H., Merzouki, A., Pacheco, A., 2015. Estimation of Leaf Area Index (LAI) in corn and soybeans using multi-polarization C-and L-band radar data. Remote Sensing of Environment 170, 77–89.
25. Jia, Q., Wang, Y.-P., 2021. Relationships between leaf area index and evapotranspiration and crop coefficient of hilly apple orchard in the Loess Plateau. Water 13, 1957.
26. Jin, X., Kumar, L., Li, Z., Feng, H., Xu, X., Yang, G., Wang, J., 2018. A review of data assimilation of remote sensing and crop models. Eur. J. Agron. 92, 141–152.
27. Jones, J.W., Hoogenboom, G., Porter, C.H., Boote, K.J., Batchelor, W.D., Hunt, L., Wilkens, P.W., Singh, U., Gijsman, A.J., Ritchie, J.T., 2003. The DSSAT cropping system model. Eur. J. Agron. 18, 235–265.
28. Kannan, S., Kaliaperumal, R., Pazhanivelan, S., Kumaraperumal, R., Sivakumar, K., 2021a. Paddy area estimation in Nagapattinam district using sentinel-1A SAR data. Pharma Innov. J. 10, 112–116.
29. Kannan, S., Kaliaperumal, R., Pazhanivelan, S., Kumaraperumal, R., Sivakumar, K., 2021b. Paddy area estimation in Nagapattinam district using sentinel-1A SAR data. Pharma Innov. J. 10, 112–116.
30. Karydas, C.G., Toukiloglou, P., Minakou, C., Gitas, I.Z., 2015. Development of a rule-based algorithm for rice cultivation mapping using Landsat 8 time series, in: Hadjimitsis, D.G., Themistocleous, K., Michaelides, S., Papadavid, G. (Eds.), . Presented at the Third International Conference on Remote Sensing and Geoinformation of the Environment, Paphos, Cyprus, p. 95350K. https://doi.org/10.1117/12.2193162
31. Khobragade, A., Jadhav, J., Londhe, V., Jadhav, V., Sthool, V., Bagade, S., Rathod, A., 2023. Simulation and validation using InfoCrop model for Rabi sorghum crop under scarcity zone of India.

32. Kumar, A., Tripathi, P., Yadav, S., Singh, K., Mishra, S., 2015. Validation of InfoCrop model for rice cultivar under eastern plain zone of Uttar Pradesh. J. Agrometeorol. 17, 80–83.
33. Kumar, A.A., Anuradha, K., Ramaiah, B., Grando, S., Frederick, H., Rattunde, W., Virk, P., Pfeiffer, W.H., 2015. Recent Advances in Sorghum Biofortification Research, in: Janick, J. (Ed.), Plant Breeding Reviews: Volume 39. Wiley, pp. 89–124. https://doi.org/10.1002/9781119107743.ch03
34. Leite, R., Amorim, L., Bergamin Filho, A., 2006. Relationships of disease and leaf area variables with yield in the Alternaria helianthi–sunflower pathosystem. Plant Pathology 55, 73–81.
35. Li, H., Liu, Z., Chen, Y., Zhang, X., Chen, D., 2022. A positive correlation between seed cotton yield and high-efficiency leaf area index in directly seeded short-season cotton after wheat. Field Crops Research 285, 108594.
36. Li, T., Humphreys, E., Gill, G., Kukal, S., 2011. Evaluation and application of ORYZA2000 for irrigation scheduling of puddled transplanted rice in north west India. Field Crops Res. 122, 104–117.
37. Liu, C., Chen, Z.-X., Yun, S., Chen, J., Hasi, T., PAN, H., 2019. Research advances of SAR remote sensing for agriculture applications: A review. J. Integr. Agric. 18, 506–525.
38. LIU, X., Qiang, C., YUAN, Z., Xia, L., WANG, X., TIAN, Y., CAO, W., Yan, Z., 2018. Leaf area index-based nitrogen diagnosis in irrigated lowland rice. Journal of integrative agriculture 17, 111–121.
39. Lobell, D.B., Burke, M.B., 2010. On the use of statistical models to predict crop yield responses to climate change. Agric. For. Meteorol. 150, 1443–1452.
40. Lobell, D.B., Thau, D., Seifert, C., Engle, E., Little, B., 2015. A scalable satellite-based crop yield mapper. Remote Sens. Environ. 164, 324–333.
41. Mohanty, M., Probert, M., Reddy, K.S., Dalal, R., Mishra, A., Rao, A.S., Singh, M., Menzies, N., 2012. Simulating soybean–wheat cropping system: APSIM model parameterization and validation. Agric. Ecosyst. Environ. 152, 68–78.
42. Mosleh, M., Hassan, Q., Chowdhury, E., 2015. Application of Remote Sensors in Mapping Rice Area and Forecasting Its Production: A Review. Sensors 15, 769–791. https://doi.org/10.3390/s150100769
43. Murthy, C., Raju, P., Badrinath, K., 2003. Classification of wheat crop with multi-temporal images: Performance of maximum likelihood and artificial neural networks. Int. J. Remote Sens. 24, 4871–4890.
44. Murty, M., Singh, P., Wani, S., Khairwal, I., Srinivas, K., 2007. Yield gap analysis of sorghum and pearl millet in India using simulation modeling.
45. Nagaleekara, B., Patil, R., Sumesh, K., 2023. Irrigation as an adaptation strategy to cope with climate change in kharif sorghum hybrid CSH-16 across 12 districts of north interior Karnataka.
46. Naresh Kumar, S., Aggarwal, P., Swaroopa Rani, D., Saxena, R., Chauhan, N., Jain, S., 2014. Vulnerability of wheat production to climate change in India. Clim. Res. 59, 173–187. https://doi.org/10.3354/cr01212

47. NASA Langley Research Center Atmospheric Science Data Center (2021-22). POWER (Prediction of Worldwide Energy Resource) Data. NASA POWER Project Data Archive. https://power.larc.nasa.gov/
48. Nearing, G.S., Crow, W.T., Thorp, K.R., Moran, M.S., Reichle, R.H., Gupta, H.V., 2012. Assimilating remote sensing observations of leaf area index and soil moisture for wheat yield estimates: An observing system simulation experiment. Water Resour. Res. 48, 2011WR011420. https://doi.org/10.1029/2011WR011420
49. Pandya, M.R., Singh, R.P., Chaudhari, K.N., Bairagi, G.D., Sharma, R., Dadhwal, V.K., Parihar, J.S., 2006. Leaf area index retrieval using IRS LISS-III sensor data and validation of the MODIS LAI product over central India. IEEE Trans. Geosci. Remote Sens. 44, 1858–1865. https://doi.org/10.1109/TGRS.2006.876028
50. Parag, M., Lottering, R., Peerbhay, K., Agjee, N., Poona, N., 2023. The use of synthetic aperture radar technology for crop biomass monitoring: A systematic review. Remote Sens. Appl. Soc. Environ. 101107.
51. Parmar, P., Patel, H.R., Yadav, S.B., Pandey, V., 2013. Calibration and validation of DSSAT model for kharif groundnut in north-Saurashtra agro-climatic zone of Gujarat. J. Agrometeorol. 15, 62–65.
52. Pazhanivelan, S., Geethalakshmi, V., Tamilmounika, R., Sudarmanian, N., Kaliaperumal, R., Ramalingam, K., Sivamurugan, A., Mrunalini, K., Yadav, M.K., Quicho, E.D., 2022. Spatial rice yield estimation using multiple linear regression analysis, semi-physical approach and assimilating SAR satellite derived products with DSSAT crop simulation model. Agronomy 12, 2008.
53. Potdar, M., 1993. Sorghum yield modelling based on crop growth parameters determined from visible and near-IR channel NOAA AVHRR data. Int. J. Remote Sens. 14, 895–905.
54. Potgieter, A.B., Zhao, Y., Zarco-Tejada, P.J., Chenu, K., Zhang, Y., Porker, K., Biddulph, B., Dang, Y.P., Neale, T., Roosta, F., 2021. Evolution and application of digital technologies to predict crop type and crop phenology in agriculture. Silico Plants 3, diab017.
55. Quarmby, N.A., Milnes, M., Hindle, T.L., Silleos, N., 1993. The use of multi-temporal NDVI measurements from AVHRR data for crop yield estimation and prediction. Int. J. Remote Sens. 14, 199–210. https://doi.org/10.1080/01431169308904332
56. Ragunath Kaliaperumal, S.K., R. Kumaraperumal, S.P., Sivakumar, K., 2021. Rice Area Estimation using Sentinel 1A SAR Data in Cauvery Delta Region. Int. J. Curr. Microbiol. Appl. Sci. 10, 848–853. https://doi.org/10.20546/ijcmas.2021.1002.100
57. Raviz, J., Mabalay, M.R., Laborte, A., Nelson, A., Holecz, F., Quilang, E.J., Barbieri, M., De Dios, J., Collivignarelli, F., Gatti, L., 2015. Mapping rice areas in Mindanao using the first images from Sentinel-1A: The PRISM Project experience. Presented at the 36th Asian Conference on Remote Sensing (ACRS), Manila, October, Citeseer, pp. 19–23.
58. Sandeep, V., Rao, B.B., Bharathi, G., Rao, V., Pramod, V., Chowdary, P., Patel, N., Kumar, P.V., 2017. Projecting future changes in water requirement of grain sorghum in India. J. Agrometeorol. 19, 217–225.

59. Sandeep, V., Rao, V., Rao, B.B., Pramod, V., Chowdary, P.S., Kumar, P.V., BHARATHI, G., PATEL, N., MUKESH, P., 2018. Impact of climate change on sorghum productivity in India and its adaptation strategies. J. Agrometeorol. 20, 89–96.
60. Satheesh, S., Pazhanivelan, S., Kumaraperumal, R., Radhamani, S., Ragunath, K., Sudarmanian, N., 2022. Area Assessment for Rice Crop in Thiruvarur District Assimilating Sentinel 1A Satellite Data. Int. J. Environ. Clim. Change 12, 1270–1278.
61. Saxena, S., Dubey, S., Choudhary, K., Sehgal, S., Ray, S., 2019. An analysis of national-state-district level acreage and production estimates of Rabi Sorghum under Fasal project. Int. Arch. Photogramm. Remote Sens. Spat. Inf. Sci. 42, 79–84.
62. Selvaraju, N., Ragunath, K., Pazhanivelan, S., Kannan, B., 2019. Mapping of sugarcane area using sentinel 1a SAR satellite data.
63. Setiyono, T., Quicho, E., Holecz, F., Khan, N., Romuga, G., Maunahan, A., Garcia, C., Rala, A., Raviz, J., Collivignarelli, F., 2019. Rice yield estimation using synthetic aperture radar (SAR) and the ORYZA crop growth model: development and application of the system in South and South-east Asian countries. Int. J. Remote Sens. 40, 8093–8124.
64. Singh, A., Saha, S., Mondal, S., 2013. Modelling irrigated wheat production using the FAO AquaCrop model in West Bengal, India, for sustainable agriculture. Irrig. Drain. 62, 50–56.
65. Singh, P., Singh, K., Bhan, S., Baxla, A., Singh, S., Rathore, L., Gupta, A., 2017. Impact of projected climate change on rice (Oryza sativa L.) yield using CERES-rice model in different agroclimatic zones of India. Curr. Sci. 108–115.
66. Srivastava, A., Kumar, S.N., Aggarwal, P.K., 2010. Assessment on vulnerability of sorghum to climate change in India. Agric. Ecosyst. Environ. 138, 160–169.
67. Su, L., Wang, Q., Wang, C., Shan, Y., 2015. Simulation models of leaf area index and yield for cotton grown with different soil conditioners. PLoS One 10, e0141835.
68. Subash, N., Mohan, H.R., 2012. Evaluation of the impact of climatic trends and variability in rice–wheat system productivity using Cropping System Model DSSAT over the Indo-Gangetic Plains of India. Agric. For. Meteorol. 164, 71–81.
69. Thirumeninathan, S., Pazhanivelan, S., Sudarmanian, N., Ragunath, K., Kumaraperumal, R., Srinivasan, G., Mohan, R., 2023. Integrating SAR Sentinel-1A and DSSAT CROPGRO Simulation Model for Peanut Yield Gap Analysis. Agronomy 13, 889.
70. Umesh, B., Reddy, K., Polisgowdar, B., Maruthi, V., Satishkumar, U., Ayyanagoudar, M., Rao, S., Veeresh, H., 2022. Assessment of climate change impact on maize (Zea mays L.) through aquacrop model in semi-arid alfisol of southern Telangana. Agric. Water Manag. 274, 107950.
71. Wagner, M.P., Slawig, T., Taravat, A., Oppelt, N., 2020. Remote sensing data assimilation in dynamic crop models using particle swarm optimization. ISPRS Int. J. Geo-Inf. 9, 105.
72. Yadav, S., Patel, H., Patel, G., Lunagaria, M., Karande, B., Shah, A., Pandey, V., 2012. Calibration and validation of PNUTGRO (DSSAT v4. 5) model for yield and yield attributing characters of kharif groundnut cultivars in middle Gujarat region. J Agrometeorol Spec. 14, 24–9.

73. Zhou, X., Zheng, H., Xu, X., He, J., Ge, X., Yao, X., Cheng, T., Zhu, Y., Cao, W., Tian, Y., 2017. Predicting grain yield in rice using multi-temporal vegetation indices from UAV-based multispectral and digital imagery. ISPRS J. Photogramm. Remote Sens. 130, 246–255.

Figures

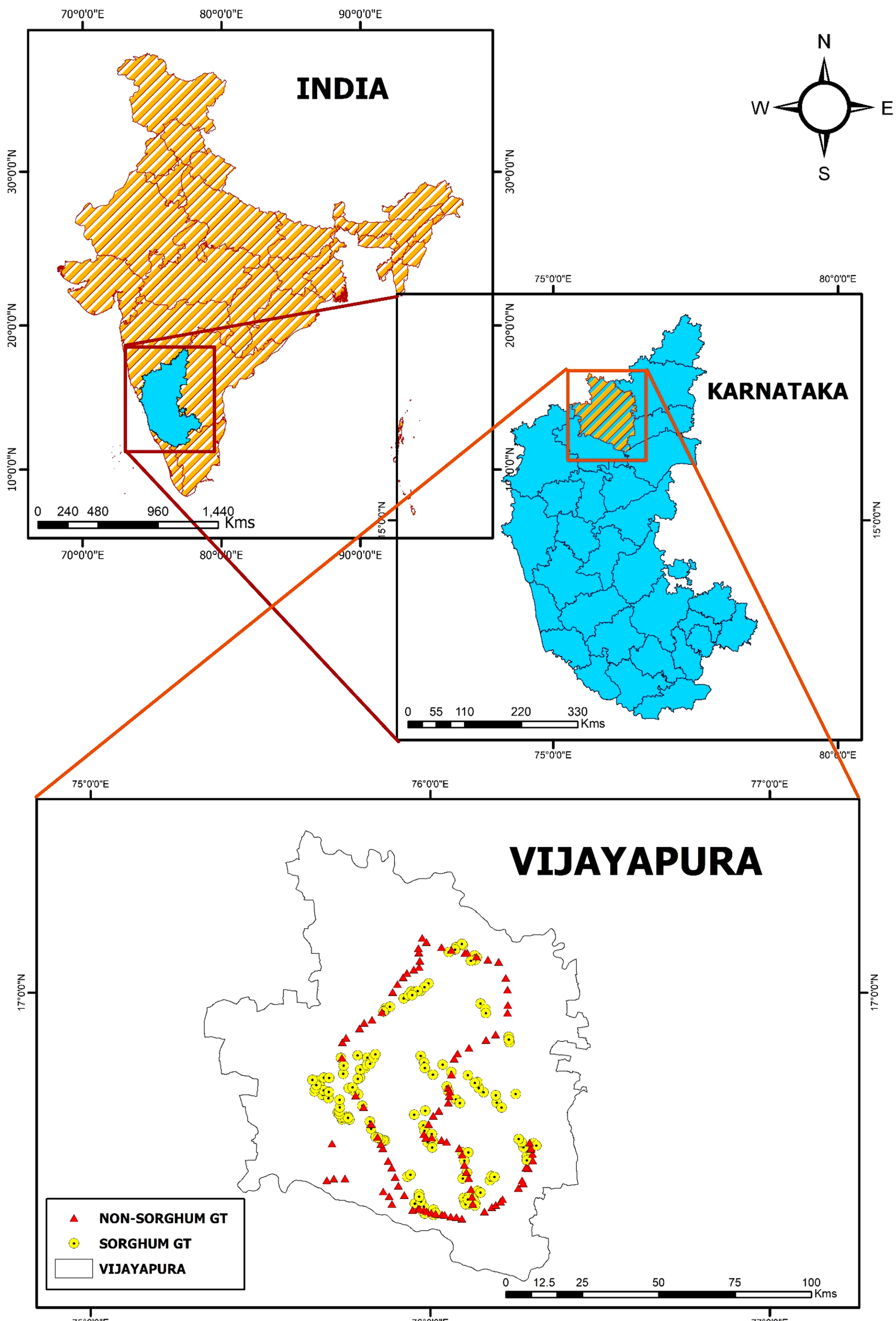

Figure 1

Map depicting the study area along with GT points.

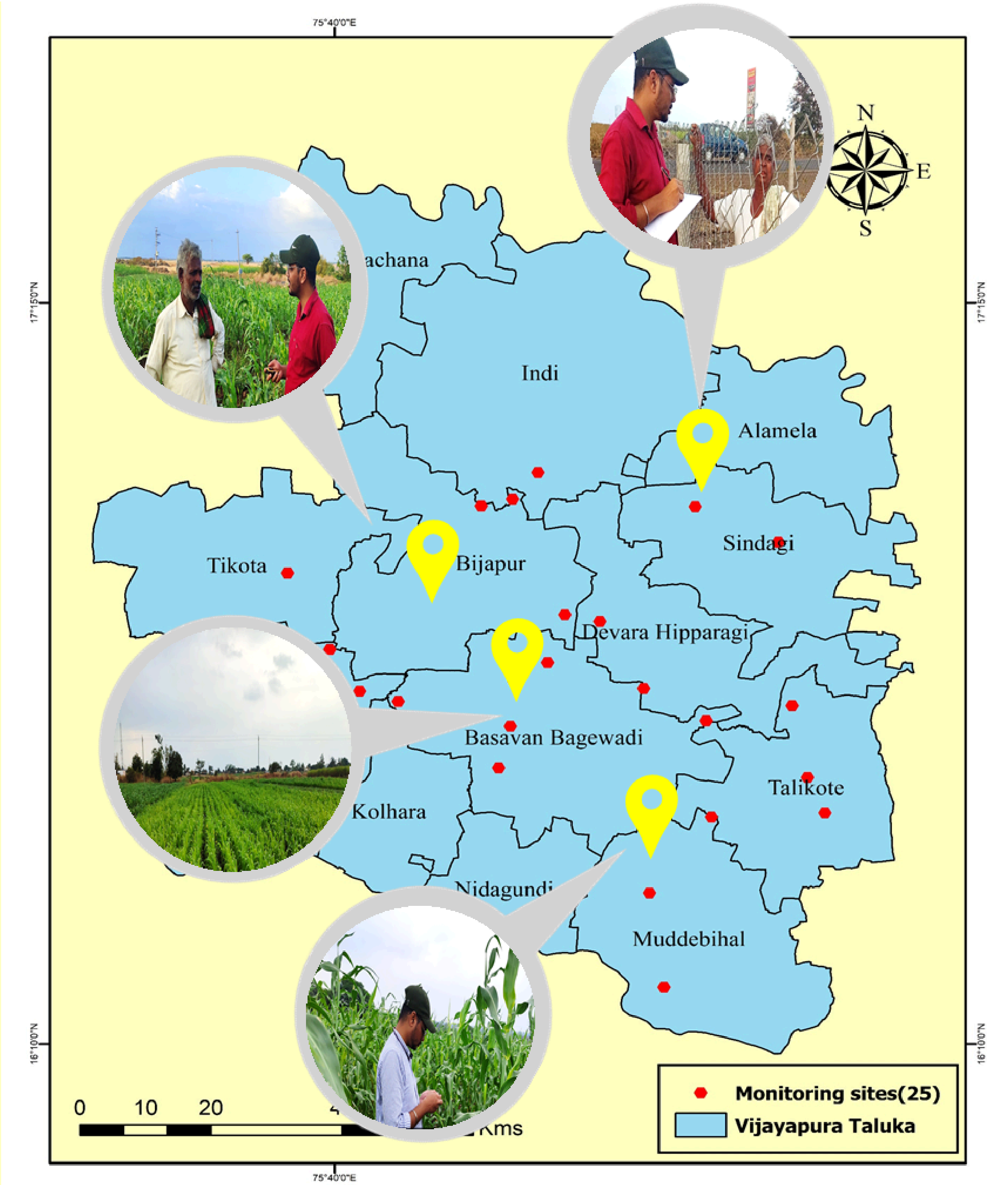

Figure 2

Flow chart of the methodology for the area and yield using SAR and CSM models.

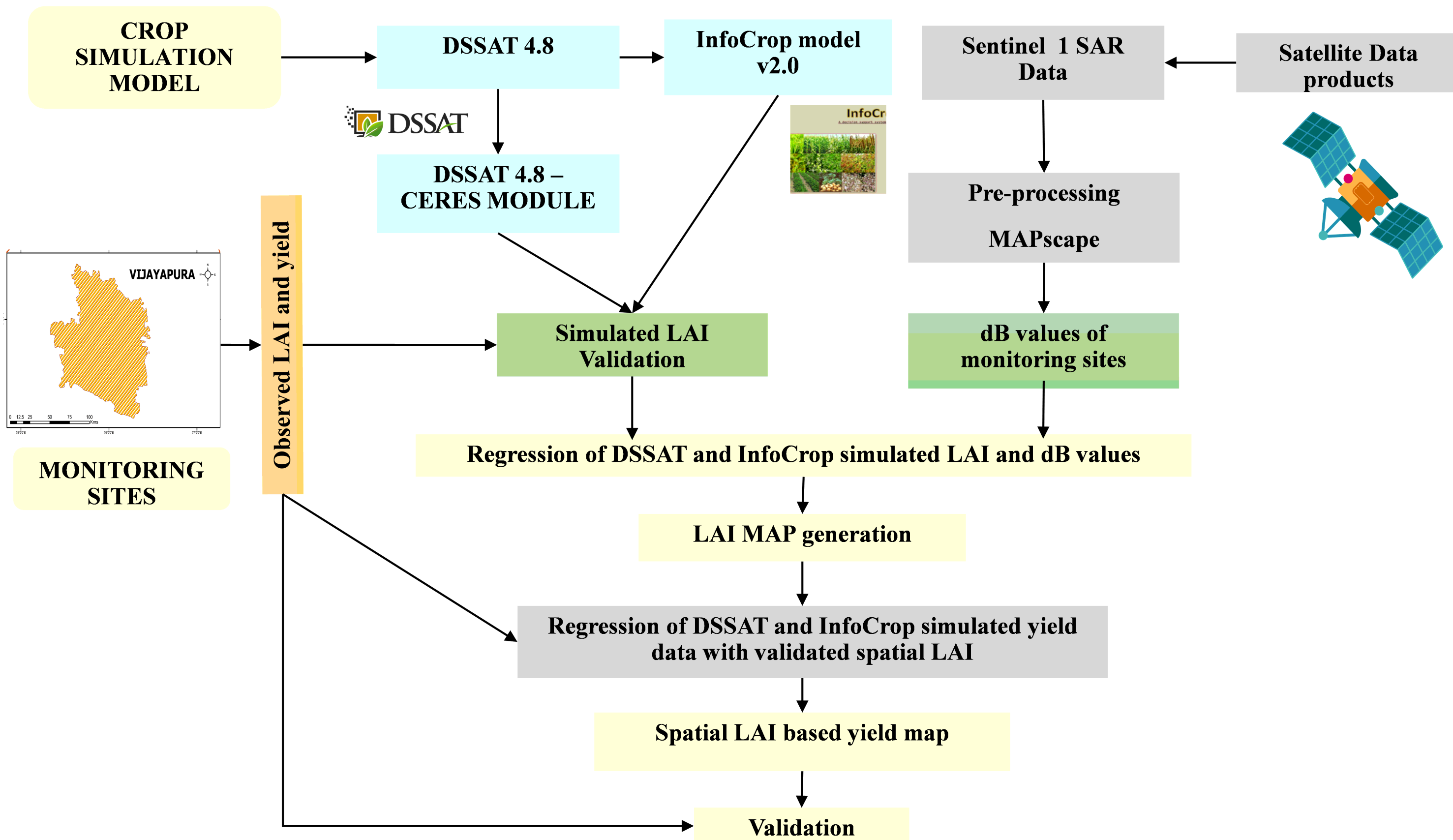

Figure 3

illustrations data collection of monitoring locations-based on block-level approach in Vijayapura, Karnataka

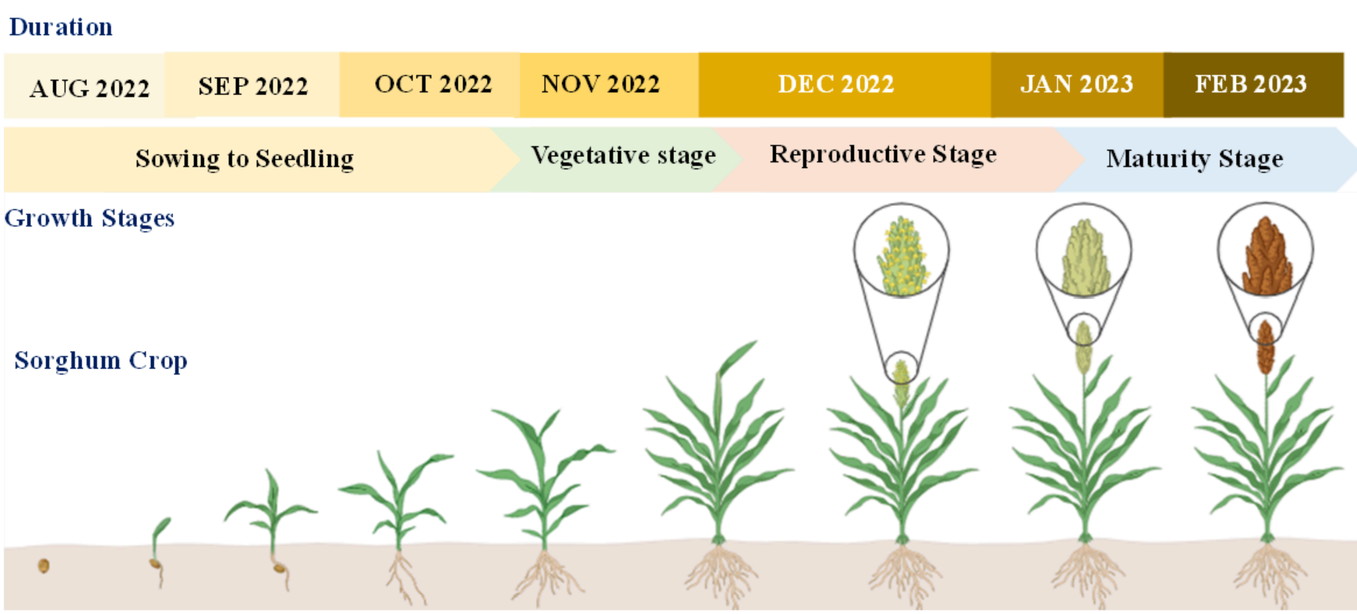

Figure 4

Crop calendar of Rabi Sorghum in Vijayapura

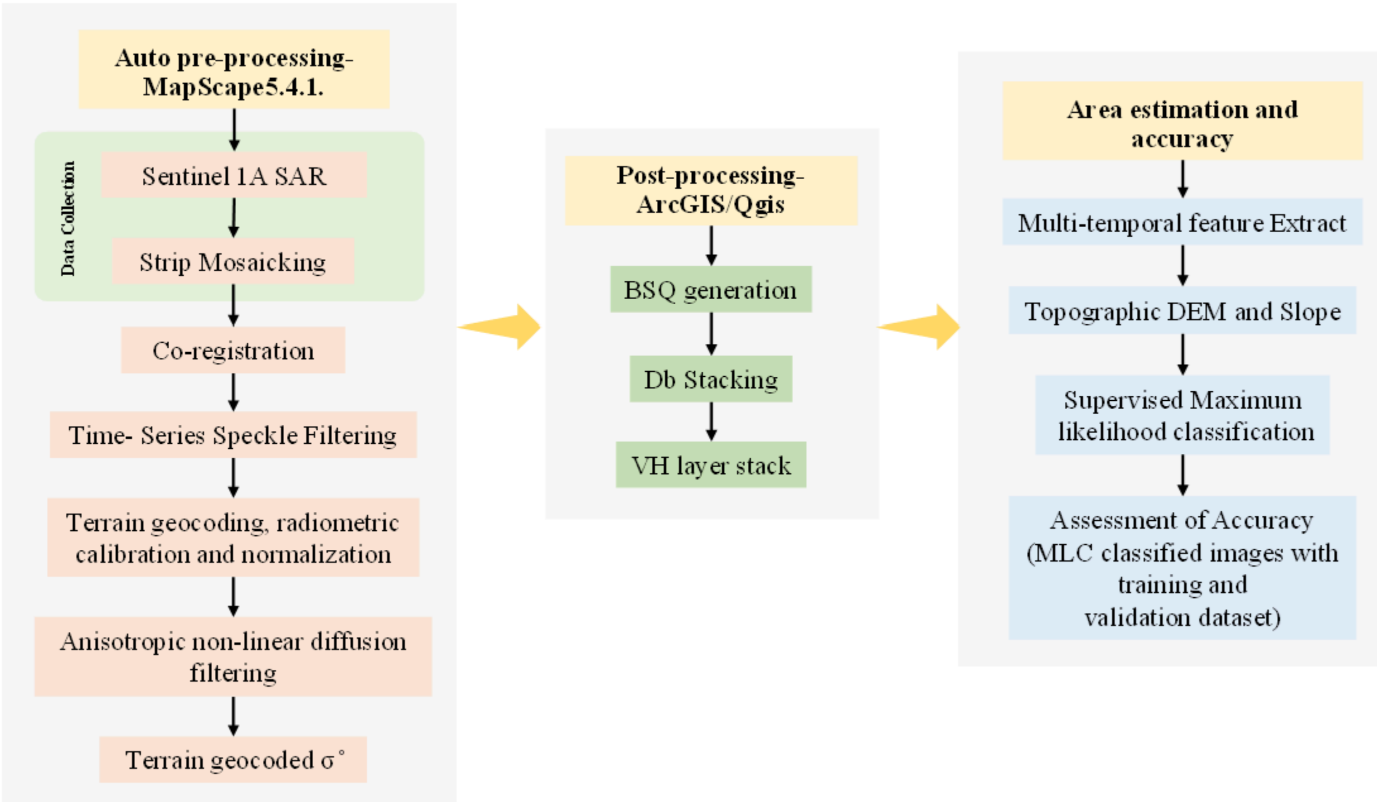

Figure 5

Flow chart depicting the sorghum area mapping methodology

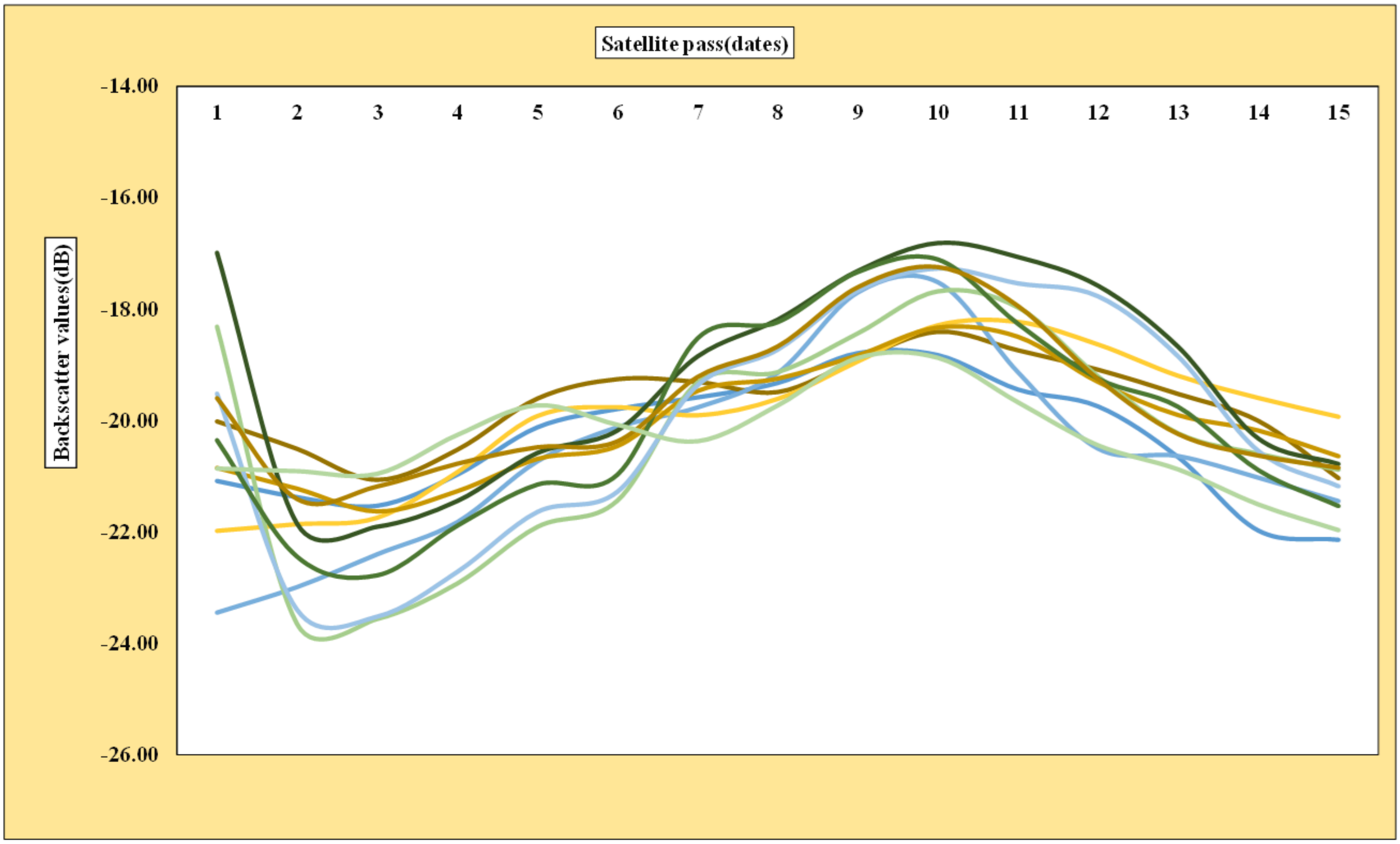

Figure 6

VH polarization dB curve for monitoring Rabi sorghum sites.

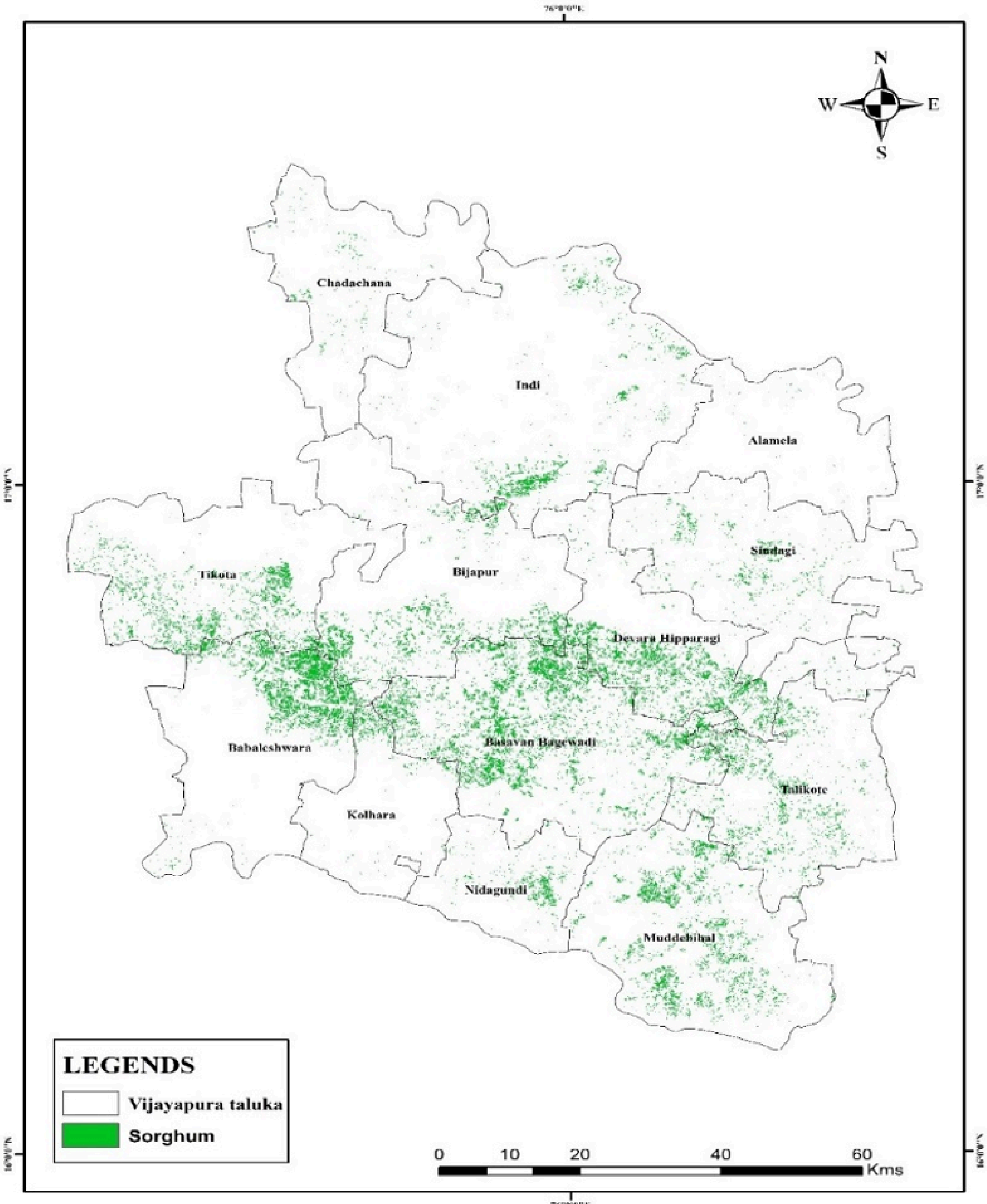

Figure 7

Map depicting the rabi sorghum in the study area

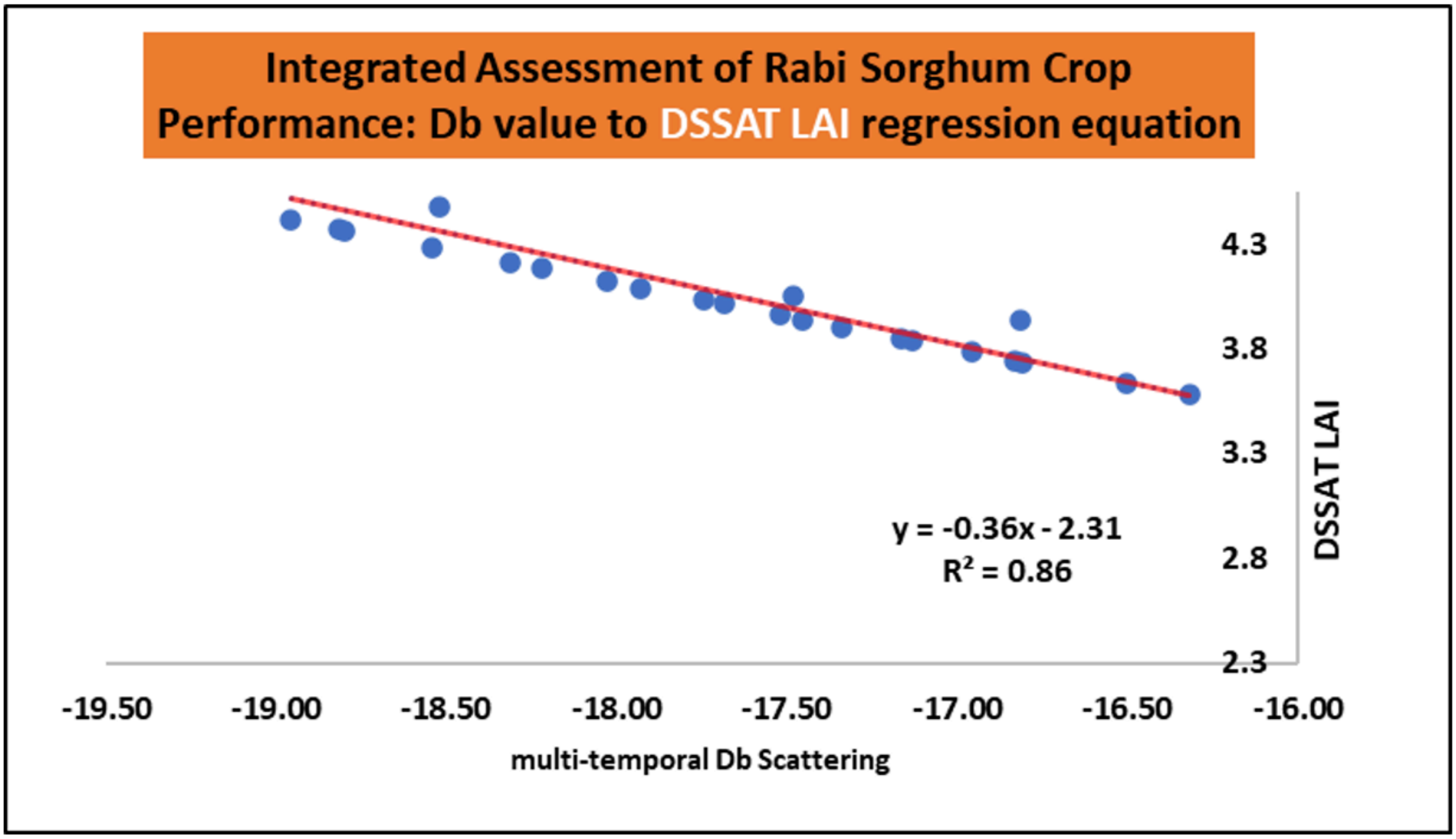

Figure 8

Scatterplots of dB value and DSSAT simulated LAI

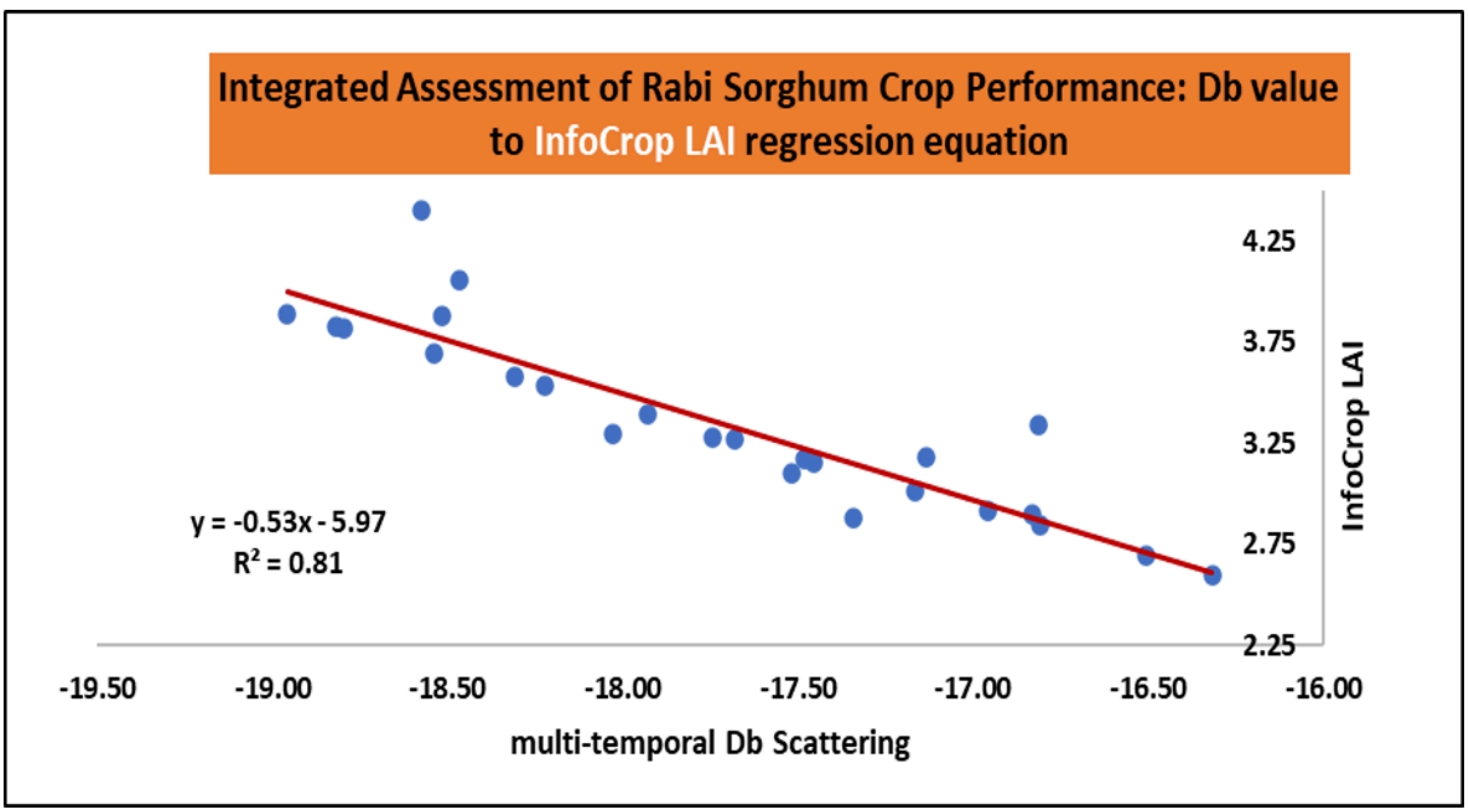

Figure 9

Scatterplots of dB value and InfoCrop simulated LAI

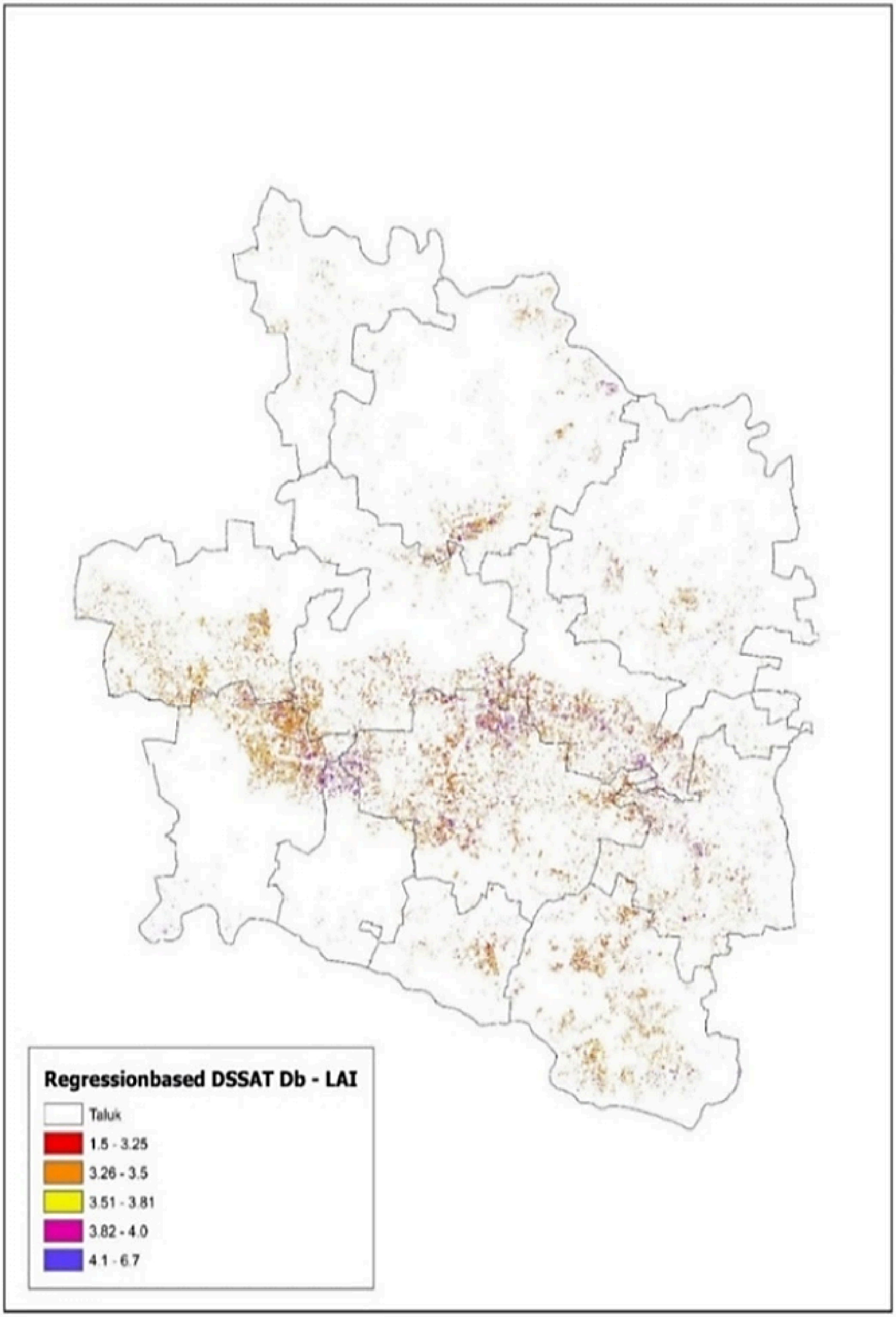

Figure 10

Depiction of LAI map (Db-DSSAT LAI)

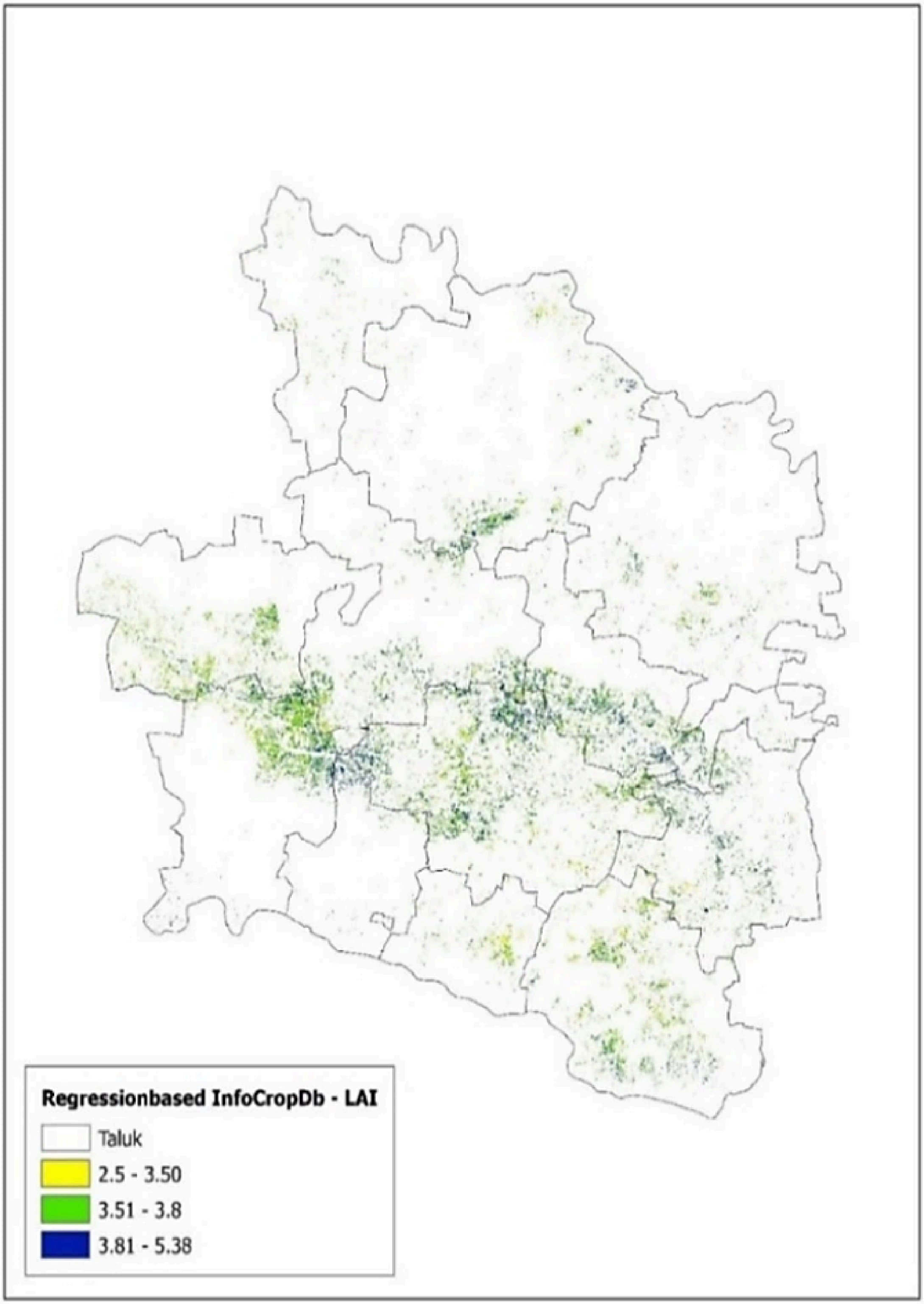

Figure 11

Depiction of LAI map (Db-InfoCrop LAI)

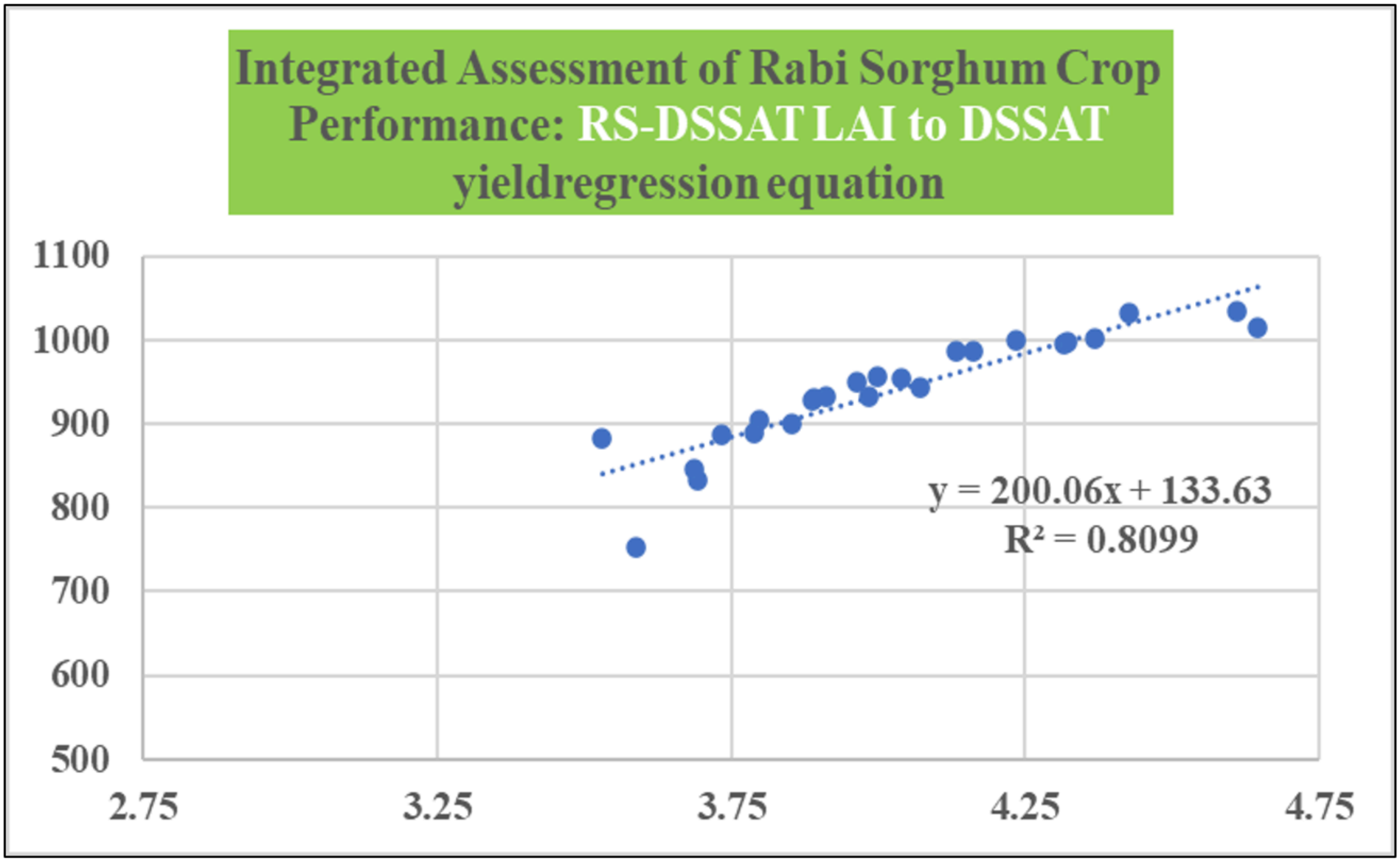

Figure 12

Scatterplots of Spatial LAI and DSSAT yield

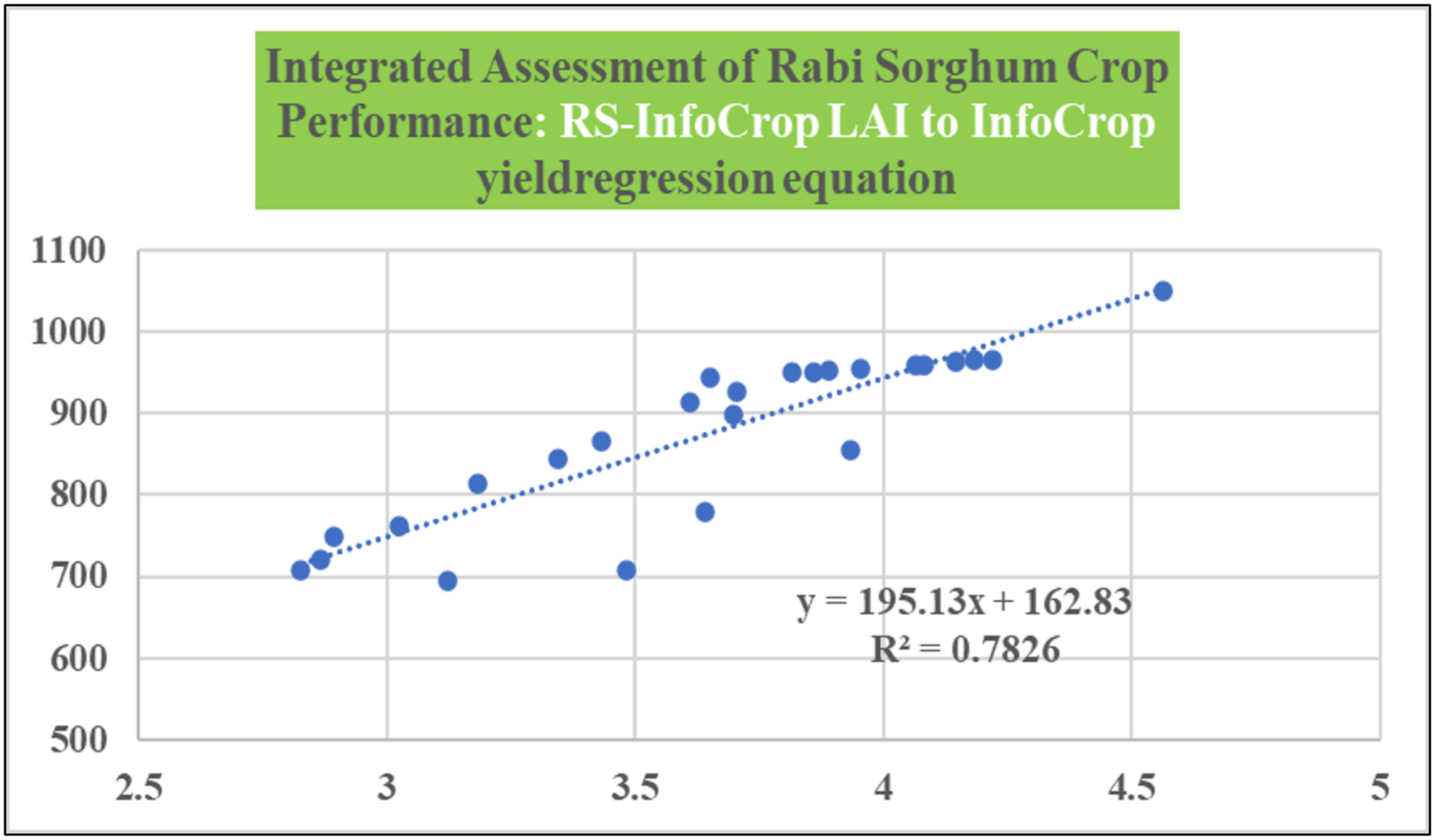

Figure 13

Scatterplots of Spatial LAI and InfoCrop yield

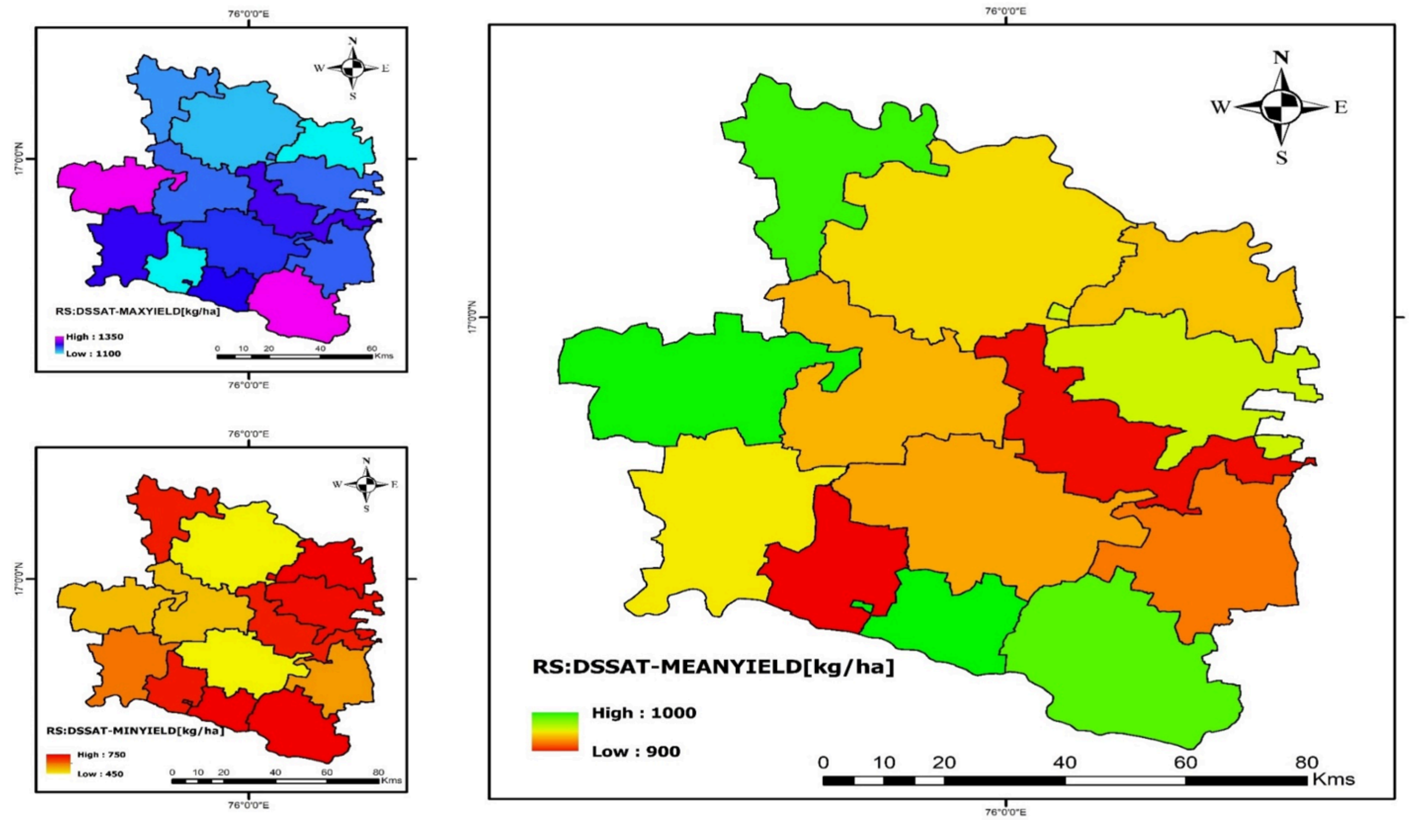

Figure 14

Depiction of yield- map (RS: DSSAT LAI – DSSAT simulated yield)

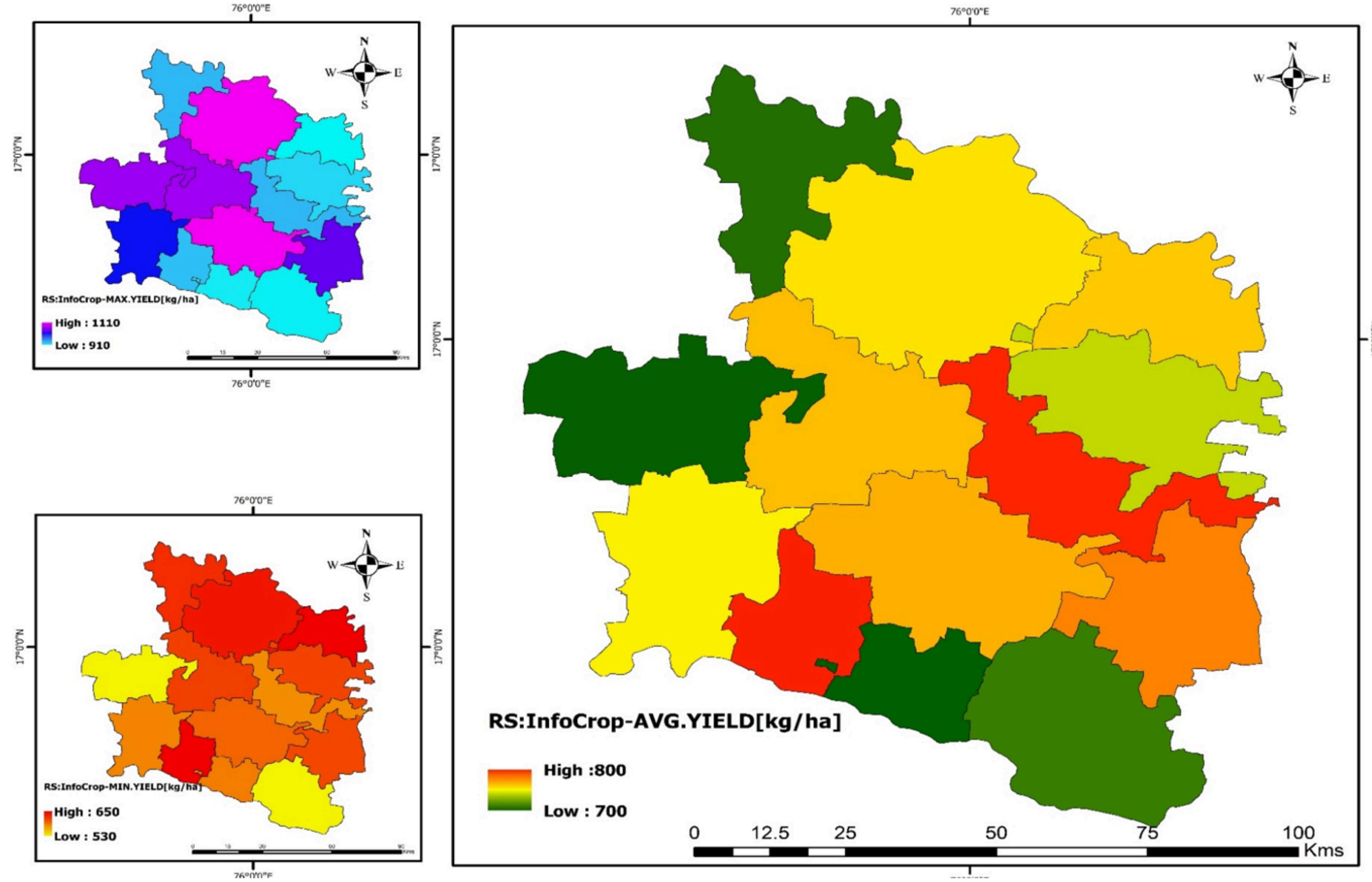

Figure 15

Depiction of yield- map (RS: Info Crop LAI – Info Crop simulated yield)

Supplementary Files

This is a list of supplementary files associated with this preprint. Click to download.

- GraphicalAbstract.docx